ELECTRICAL CONDUCTIVITY MEASUREMENTS ON ICE CORES FROM THE CANADIAN ARCTIC: AN ANALYSIS OF SIGNAL VARIATION WITHIN AND BETWEEN ICE CORES

by

Jiancheng Zheng

A Thesis Submitted to the School of Graduate Studies and Research

in partial fulfilment of the requirements

for the degree of M. Sc. in Earth Sciences

OTTAWA-CARLETON GEOSCIENCE CENTRE

AND

UNIVERSITY OF OTTAWA

OTTAWA, CANADA

ISBN 0-612-15690-7

UNIVERSITÉ D'OTTAWA
UNIVERSITY OF OTTAWA

Acknowledgements

I sincerely thank Professor Ian D. Clark at the University of Ottawa, Dr. Akira Kudo at the National Research Council of Canada and Dr. David A. Fisher at the National Resources of Canada, who created an opportunity for me to get into the Master program.

As my thesis supervisor, Professor Ian D. Clark has been guiding me in the last three years. I remember the first time when I visited his office. He told me to give him a call or go to see him whenever I need help. He did what he said. Not only in the classrooms or in the labs, but also in his office, even after the working hours, Professor Clark always very kindly explained me all my questions, gave me his suggestions and helped to carefully modify this thesis.

As my working supervisor, Dr. Akira Kudo delicately arranged my working time so that I could have time to finish my courses. Dr. Kudo also helped to design the ECM scanning system; and to innovatively design the independent electrode system for the ECM system, which has been proved to be practical and accurate.

Dr. David Fisher, my teacher, colleague and friend, has been helping me since the very beginning of my getting into my master program. Without his help, I would never have got

this thesis to this stage both academically and technically. The deepest impression he gave me was during the 1993 field trip on Agassiz Ice Cap. At that trip, he was the chief (coordinating the whole group of 12 people with different projects), the professor (coaching almost everyone from drilling technology to glacial sciences), the hard worker (working about 15 hours a day everyday) and the breakfast cook (making pancakes for everybody starting at 5 am everyday). I remember that I, one day, asked him why he got up so early everyday (It is very hard for me to get up so early) and he told me his cat help him to get used to getting up early because the cat had very precisely wakened him at 5 am for many years. I wish I could be lucky enough to get a similar cat to help me be a little bit more industrious.

The author is indebted to Dr. Don Singleton at the National Research Council of Canada, Dr. Roy M. Koerner at the National resources of Canada, and Professor Michel J. Robin and Professor Anthony D. Fowler at the University of Ottawa, and Professor C. R. Burn at the Carleton University for their nice discussions, suggestions and/or modifications of this thesis; Dr. Erik Blake in the Ice Field Instruments Ltd. for his kindly supporting me part of the ECM data used in this thesis, Mr. Van Luong in the National Research Council of Canada who helped design the system controling component for the ECM system; Mr. John Woods at the National Research Council of Canada who analysed the Anion samples. Thanks also goes to Miss Isabelle Cayer for the English correction and Dr.Paul Barrette for the abstract translation from English to French and his nice discussion on part of this thesis.

Abstract

Two ice cores, A93.1 and A93.2, drilled two meters apart at the Agassiz Ice Cap in May of 1993, had on site electrical conductivity measurements (ECM) carried out to determine the confidence limits of the ECM method for chronological and stratigraphic control. Four ECM profiles have been produced from the two cores, one directly on unprepared surfaces of A93.1 and A93.2 and two on a prepared surface of the A93.1 made by a band saw and subsequently planed by a clean microtome knife. Two slightly different ECM systems were used. The two prepared surface data sets on the A93.1 gave virtually identical results. The profiles from the microtomed surface and the unprepared surface of A93.1 have a slight difference. A larger discrepancy, however, was observed between the two cores, A93.1 and A93.2.

The correlation analysis between the two ECM series of whole length ice core on A93.1 prepared and unprepared surfaces gives a correlation coefficient of 0.842, which suggests that ECM may be carried out directly on the newly mechanically recovered ice core without preparing a new surface if care is being taken during the core handling and ECM processing. Measurement on unprepared surfaces is particularly valid when quick location of some strong signal events like the Laki volcanic eruption needs to be done on site. Correlation analysis of high resolution ECM records from the A93.1 prepared

and unprepared surfaces over the last 250 years shows a 10 to 30% coefficient variability, which may be accounted for by the methodological noise and crystallography. The correlation analysis of whole length of A93.1 and A93.2 cores on the unprepared surfaces gives a coefficient of 0.644. Correlation analysis of high resolution ECM records over the last 250 years between the two cores gives a 30 to 50% coefficient variability. This suggests that there is a combined drift/melt noise contribution of 20% of coefficient variability on top of the methodological noise and crystallographic difference for cores this close together. A strong correlation between the results from the two ECM systems tested indicates that different systems are comparable if the two ECM systems are similarly designed.

Review of multi-ice core records including $\delta^{18}O$, ECM and melt percentage, shows that ice on the Agassiz Ice Cap of Canadian High Arctic is continuous from present to the earlier Holocene. However, 100% melt percentage, high $\delta^{18}O$ noise and the discontinuities of $\delta^{18}O$ in the early Holocene suggests that a gap in the stratigraphy may exist in that interval.

Résumé

Deux carottes de glace, A93.1 et A93.2, furent recueillies à un intervalle de deux mètres sur la calotte glaciaire Agassiz en mai 1993. Des essais de conductivité électrique (ECE) ont été effectués sur ces carottes, au site de forage, dans le but de déterminer les limites de confiance inhérentes à cette méthode lorsqu'appliquée à des études chronologiques et stratigraphiques. Quatre profils ECE ont été obtenus. Deux de ces profils proviennent d'une surface non préparée de A93.1 et A93.2. Deux autres ont été mesurés à partir d'une surface tranchée à l'aide d'une scie à ruban et subséquemment polie avec un couteau de microtome. Les deux derniers tests, qui comportaient une variation dans les procédures de ECE, ont offert des résultats presqu'identiques. Une plus grande divergence des données a été observée entre les tests effectués sur les surfaces non-préparées de A93.1 et A93.2.

Un facteur de correlation de 0.842 entre les deux séries de ECE (surface préparée et non-préparée) sur la longueur totale de la carotte A93.1 suggère que la préparation de la surface n'est pas essentielle si la manipulation des carottes et le traitement des données est effectuée avec soin. Une surface non préparée est particulièrement appropriée dans le cas où une localisation rapide d'un événement spécial, tel l'éruption volcanique de Laki, est requise. Une analyse de correlation à haute résolution sur les surfaces préparées

de A93.1, représentant une période de 250 ans, démontre une variance de 10 à 30%, laquelle est attribuée aux procédures d'examens et à la cristallographie de la carotte. Un coefficient de 0.644 a été obtenu à partir des surfaces préparée et non préparée de A93.1. Les ECE à haute résolution entre ces deux carottes, couvrant une période de 250 ans, sont caractérisés par une variance de 30 à 50%. Ce 20% additionel par rapport à la variance précédente pourrait, compte tenu de la proximité des sites d'échantillonage, représenter l'apport de l'effet de dérive et de fonte. Une forte correlation entre les deux méthodes utilisées pour les ECE indique un indice de performance comparable entre les deux méthodes, à condition que leur instrumentation soit de conception similaire.

Un rappel bibliographique de données provenant de la calotte glaciaire de Agassiz, comprenant $\delta^{18}O$, ECE et la fraction de fonte, démontre que son existence remonte à l'Holocène inférieur. Toutefois, une fraction de 100% de fonte, un taux élevé de bruit de fond en $\delta^{18}O$ ainsi qu'une discontinuité dans les valeurs de $\delta^{18}O$ milite en faveur d'une lacune stratigraphique dans la région de l'Holocène.

Table of content

List of Tables

List of Figures

1. Introduction

1.1 Background to ice core chemistry and electrical conductivity

Nature and climate are continually changing and leaving behind records of its physical, chemical and biological interactions. This is the basis on which palaeoenvironments can be reconstructed. Some of the better recognized sources of paleoenvironmental information include sea sediments, lake and bog deposits, tree-rings, periglacial features and ice. Among them, glacier ice has been of special importance. Ice caps are essentially products of atmospheric processes and important components of the Earth's air/sea/land/climatic system. Ample evidence shows that throughout much of the Earth's history, glacial epochs recurred at various times. The most recent glacial epoch, the Pleistocene, began about the last 2 to 3 million years ago. In the northern hemisphere, there were at least seven or eight major ice advances during the past 700,000 years (Lowe, 1984).

Recent studies on deep ice cores from both Greenland and Antarctica reinforce the view that the Pleistocene Epoch terminated by rapid deglaciation in both the northern and southern hemispheres at about the same time some 11, 550 years ago. The transition time may only be a few decades or less (Dansgaard et al., 1989, Johnsen et al., 1992 and Alley

et al., 1993). Understanding such a large temperature shift over a short transition period could be a serious challenge. It is important to better understand the palaeoclimates in order to predict future climate trends.

The waxing and waning of ice sheets and glaciers have significant effects on global climate. Glaciers are semi-closed reservoirs for atmospherically produced or transported substances. A variety of aerosol particles, volcanic dusts and acids, solid and soluble particulate matter, natural and artificial radioactive and stable isotopes, greenhouse gases, pesticides, anthropogenic chemicals and other trace substances are preserved in the ice sheets and glaciers by snow fall. This provides both short and long term records of environmental evolution, making glaciers one of the best natural libraries for environmental history.

Natural and anthropogenic compounds may directly be introduced into the atmosphere (gaseous components) or may be suspended in the atmosphere and clouds (aerosols or particles) by wind action. A portion of this material falls back onto local ground when atmospheric conditions change; part of it returns to the source area with local rain and snow. However, a portion of the material remains in the atmosphere and can be circulated to remote high latitude areas, such as the Poles and Greenland, to be deposited on glaciers with snow fall. Therefore, traces of human and natural activities may be

found in the remote ice caps, though some of the signals may be very weak, due to physical processing and possible chemical reactions during burial and diagenesis.

Ice cores recovered from anywhere in the world contain ultra-fine particles and ionic species, which demonstrates that the transport and nucleation of gases and the diffusive transport of aerosols is a regular practice of the world circulation system. The source of the ultra-fine particles and ionic species can be world-wide. They can be from soils, oceans, gas-to-particle conversions, volcanoes, anthropogenic sources or even cosmic dust.

It is estimated that the mechanism of wind erosion is responsible for injecting an estimated 100 to 1,000 million tons of aerosol into the atmosphere each year. Only a minor component of this is carried over path-lengths of many thousands of kilometres (Shaw,1989). Shaw (1989) even witnessed a spectacular Gobi desert dust veil over the Hawaiian Islands. From the Mauna Loa Observatory at 3,500 m altitude, as he described, the dust veil could be seen edge-on as a dark band, but at least half of the dust was above the observatory (as deduced from optical depth measurements). The episode lasted for about ten days. Oceans also supply sea salt aerosols to the atmosphere which could amount to one billion tons per year. The other sources are relatively small.

It may reasonably be assumed (even though it may not be fully justified) that concentrations of aerosols in ice cores are proportional to their concentrations in the atmosphere when they were deposited on the glaciers (Junge, 1977; Hansen, 1994). It is also probably reasonable to assume that dust and aerosols originating from soil and ocean sources as well as those from volcanic and anthropogenic origins be closely related to the strength of the world circulation systems. On very long time scales (10^5 years), the colder the climate, the drier the air and the lower the sea level should be. Therefore, the more dust or aerosols that get into the atmosphere the less likely they are to be removed by wet scavenging (Hansson, 1994).

Explosive volcanic eruptions can also result in decadal global climatic cooling (Lamb, 1982). However, it is not certain yet whether or not the extremely large eruptions in the past ever induced global cooling sufficient to cause glacier and ice sheet expansion (Flint, 1977). It is also uncertain whether the growth and decay of Late Quaternary ice sheets and global changes in sea level may actually have triggered episodes of volcanic activity as Hall (1982) and Sejrup et al. (1989) suggested. Rampino et al. (1979) argued that Late Quaternary rapid environmental changes may have influenced the timing of volcanic eruptions. The water redistribution accompanying the glaciation and deglaciation may have accelerated or delayed volcanic activities due to isostatic readjustments. Hall (1982) suspected that rapid deglaciation may lead to the occurrence

of both faulting and volcanic activity due to the considerable changes in the stress, strain and strain rates in the bedrock. Some very large volcanic eruptions, such as Mt Katla in southern Iceland at 10,600 BP and the Glacier Peak between 12,750 and 11,250 BP in the North Cascade Range, were triggered by the rapidly thinning ice mass (Dawson, 1992). Therefore, it seems certain that there is a relationship between climate and volcanic events even though it is not certain which is the cause and which is the effect.

A volcanic eruption is the escape of magma from reservoirs beneath the surface of the Earth's crust. Volcanic eruptions are commonly accompanied by larger amount of gases, mainly SO_2 and CO_2 (Lamb, 1970). Those gases become oxidized in the atmosphere and associated with water to form acids. Large volcanoes, like Laki, Katmai and Krakatoa produce outstanding volcanic signals. Those signals can be retrieved by different methods if the events are not very old. Some violent volcanic events, like Mt. Katla, erupted over 10,000 years ago, can still be easily distinguished in favourable glaciers. Volcanic eruptions like those are accurate and reliable horizon references. Volcanic events in the recent about 500 years are relatively recorded. Some larger eruptions earlier than 500 years are also precisely identified, such as Eldgja eruption (Iceland, 934AD) and Mazama (N.W. U.S.A., 4,400 BC) (Hammer et al., 1980).

Many methods and techniques have been adopted to the study of ice core and

palaeoclimatology. Some are designed to extract a palaeoclimatic signal (changes in environment) while others are used for developing a chronology in the ice. Electrical conductivity is one signal that can be used for both objectives. Actually, electrical conductivity has become a popular method for ice core dating (Taylor et al, 1992; 1993 and Fisher et al, 1995), especially for locating volcanic events in the field because of its fast, high resolution and convenience (Taylor et al., 1992 and Taylor et al., 1993). It is becoming one of the standard methods for ice core research. Electrical conductivity measurements (ECM) can offer high spatial resolution and are suitable for fast on-site applications. Ice core electrical conductivity is a measure of electrical current passing through an ice core under a constant voltage and reflects the ice core's total ionic chemistry. The current is proportional to the concentration of strong acids in the ice core, mainly sulphuric acid from volcanic events or other sources, nitric acid from atmospheric chemistry and other ions (Hammer et al., 1980, Legrand and Kirchner, 1990, Taylor et al., 1992, Bates et al., 1992 and Moore et al., 1992). ECM signals can also decrease to lower than the natural baseline when the acids are neutralized by ammonia from biomass burning and alkaline dust from terrestrial sources. These ECM signals record environmental conditions, and are affected by atmospheric circulation pattern changes. This is the basis for palaeoclimatic information found in ECM data.

Electrical conductivity measurements were first adopted by Hammer (1980) when a fixed

pair of electrodes were applied with 1250 V over a distance of one centimetre (Hammer, 1980). The electrodes moved on a microtomed ice core surface in a zig-zag at a velocity of 10 to 20 centimetres per second. The current on the electrodes was then transformed into acidity by a calibration curve of acidity-current relationship by measuring the pH on melted samples selected from the 404 metre long Crete core.

A strong contribution of alkaline, calcium carbonate rich, dust has been found in both Greenland and Canadian Arctic ice cores during the ice age (Hammer et al., 1985; Fisher and Koerner, 1986). The origin of the calcium carbonate rich alkaline material was proposed from the exposed oceanic continental shelves (Hammer et al., 1985) when the sea level is significantly lowered by the glaciation. Calcium carbonate from the continental shelves can react with the hydrogen ion in the ice core, which results in the buffering of alkaline and acidity

$$CaCO_3 + H^+ \rightarrow Ca^{2+} + HCO_3^-$$

In both Greenland and Agassiz cores, ice is generally alkaline below Holocene Epoch only with exception of a few cases where the dust concentrations are relatively low. The $\delta^{18}O$, dust and alkalinity results from Greenland and Agassiz cores are well correlated (Fisher et al., 1977; Fisher and Koerner, 1994). Referring to Shackleton's sea level variation (1987), the sea level changes match the dust and alkaline concentrations very

closely. In this aspect, the alkaline conductivity in the ice core is also reflecting the climatic change.

1.2 Objectives of this thesis

Many ice cores have been recovered from Greenland, Antarctica and Arctic for the purpose of studying their regional palaeoenvironments. ECM profiles provide a method for establishing a "working" chronology in the field to assist in sample collection and analysis. However, questions arise with respect to how well a single ECM profile records ice core stratigraphy, and how much of the data is non-reproducible. Duplicate long-ice-core sampling has not been undertaken to examine local variability in the ECM series (The local variability means the random variability caused by the surface irregularities). Are features from different nearby ice cores repeatable? How reliable are the results from an ice core? Do different methodologies affect the resulting series? Establishing such limits on practical reproducibility is very useful and important because the ECM method has become a standard tool in ice core research.

The objectives of this thesis are: (1) to statistically compare the ECM signal from prepared and unprepared ice core surfaces to evaluate the level of reliability from a single ECM record for chronological and palaeoclimatological interpretation, (2) to compare

the ECM series from sites separated by a few meters to a few kilometres, (3) to compare the similarity of ECM results from two similar ECM systems, (4) to correlate the ECM profiles with ice core chemistry, and (5) to review the palaeoclimate records of the Agassiz ice cores.

The results of three onsite ECM profiles and part of fourth ECM profile are examined for two adjacent ice cores recovered from the Agassiz Ice Cap in May, 1993. Ice core dating and palaeoclimate interpretations are made based on the two new ice cores drilled in 1993 and four ice cores drilled in 1977, 1979, 1984 and 1987 respectively from the Agassiz Ice Cap of Canada's High Arctic. Data for those ice cores drilled in 1977, 1979, 1984 and 1987 are supported by Dr. David A. Fisher and Dr. Roy M. Koerner (Fisher et al., 1983; Fisher and Koerner, 1896; Bourgeois, 1986; Fisher, 1987; Koerner et al., 1987; Fisher and Koerner, 1988; Koerner et al., 1988; Fisher, 1990; Koerner and Fisher, 1990; Fisher, 1991; Fisher, 1992a; Fisher 1992b; Fisher and Koerner, 1994; Fisher et al., 1995).

The electrical conductivity measurements of 1993 ice cores, A93.1 and A93.2, on original and on prepared surfaces were part of the tasks of the International Circum-Arctic Palaeoclimate Program (ICAPP), which is part of the Past Global Changes (PAGES) under the International Geosphere-Biosphere programme (IGBP). The primary objective of ICAPP was to integrate all ice core records across the entire Arctic region

into composite records that would define the spatial and temporal variability of climate change (Koerner, 1994).

1.3 Ice cap characteristics and bore hole details

The Queen Elizabeth Islands have an ice cover of 108,000 km^2. Most of the glaciers are located on the higher, mountainous areas of Devon, Ellesmere, and Axel Heiberg islands (Koerner, 1989).

The Agassiz ice cap covers the central part of Ellesmere Island, which is on the northeast of the Queen Elizabeth Islands (Figure 1). The maximum advance of Ellesmere Island ice was characterized by the radial expansion of glaciers from the Grant Land Mountains and the Agassiz ice cap. Agassiz ice cap is located between 79°45' and 81° N. Its surface topography is complex and there are nunataks in the highest parts. The ice cap is drained by glaciers that penetrate the surrounding mountains. The larger ones reach sea level. The ice core drilling site is at the northern part of Agassiz ice cap. It has a gently undulating surface (Fisher et al., 1983; Fisher and Koerner 1988). The first ice core drilling was carried out in 1977. Since then, a suite of bore holes have been drilled there: A77, A79, A84, A87 A93.1 and A93.2. The location of the ice cores is at 80.7° N and 73.1°W (Figure 1).

The A93 drilling site has a surface elevation of 1730 metres (above mean sea level), an ice thickness of 123.4 metres, a surface accumulation rate of about 10 cm per year and a basal temperature of -19.1 °C. A87 and A84 are within 30 m of each other at the top and the two A93 cores are about 80 m from A84. A79 is about 1.3 km down the flow line and A77 is a further 1.3 km down the flow line. The flow line starts at the top hole, A84, and goes down the ridge close to A79 and finally through A77 as shown in Figure 1. The details concerning the holes are given in Table 1. Accumulation down the flow line is discussed in Fisher et al (1995). Fisher et al., (1983) have shown that some accumulation around the central dome ridge was removed due to wi ter snow being scoured from the exposed high parts of the ice cap (Fisher et al., 1995).

Table 1. Agassiz ice core properties (Modified from Fisher et al., 1995).

Site	Eleva-tion (masl)	Accumu-lation (m/a ice)	Temp.(°C) 10m	Bottom	Thickness Avg. (m)	δ*(^{18}O) Average	Variance	Total Melt %
A84&						-27.99	0.88	5.1
A87	1730	0.098	-21.88	-19.1	127	-27.89	0.70	
A79	1700	0.115	-22.33	-19.0	139	-28.54	0.79	
A77	1670	0.175	-24.52	-16.7	338	-30.98	1.11	3.1
A93	1730	0.098	-21.88	-19.1	123			

* δ averages and variances refer to a period of 800 years starting at AD 1961 and pertain to the annual average time series.

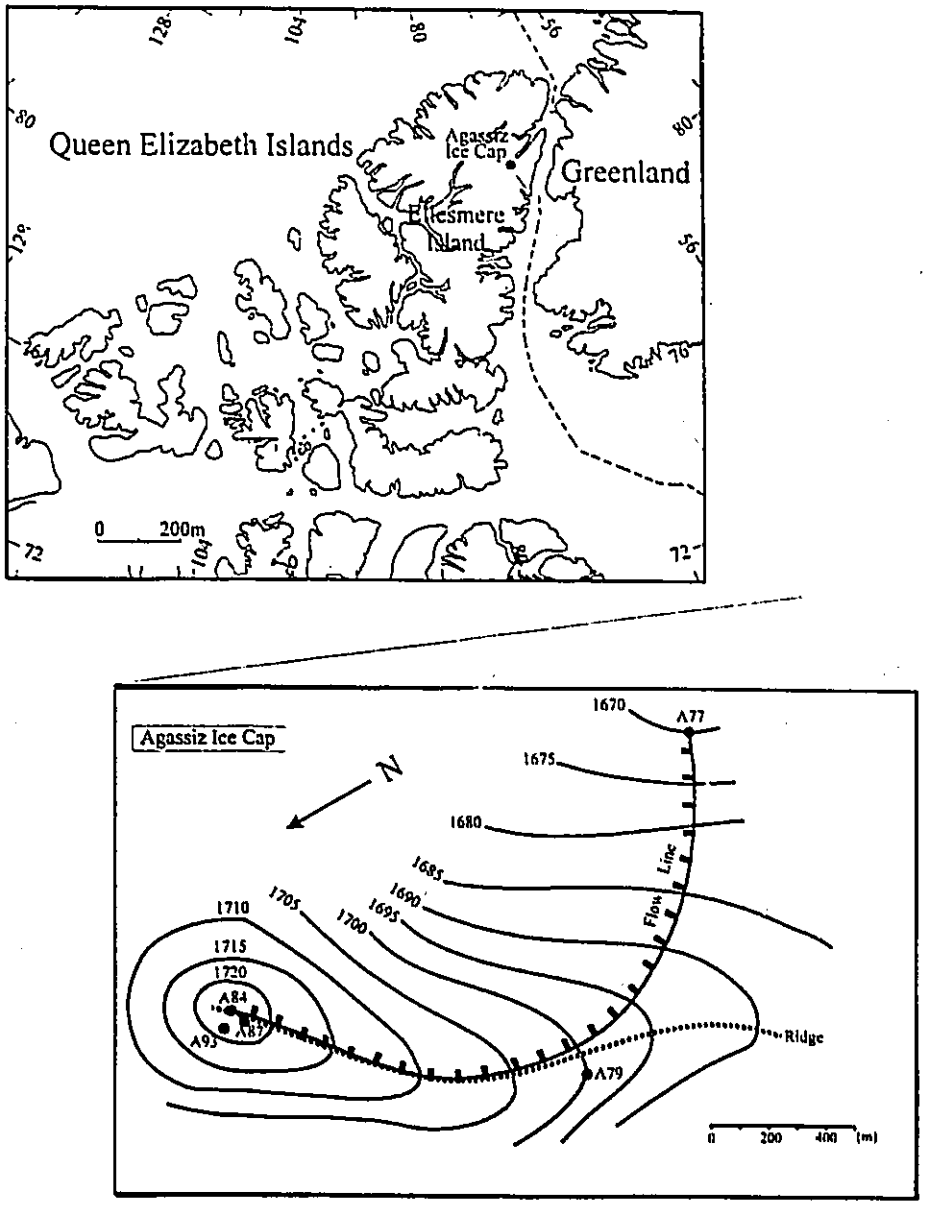

Figure 1. Map of the Agassiz bore hole sites showing the flow line from the top bore hole A84. The elevations are by levelling and are internally accurate to within 0.20 metres but could contain an absolute error of several 10s of metres (Modified from Fisher et al., 1995).

1.4 Age dating history on the Agassiz ice cores

The establishment of reliable chronologies for ice cores is a primary requirement for their interpretation as environmental and climatic records. Meanwhile, to meaningfully compare two ice core records, it is necessary to set up accurate and continuous chronologies.

To establish the age-depth relationship for an ice core, a variety of methods can be used. Precision, however, may differ for different methods. Counting physical and/or chemical annual layers; matching features of the $\delta^{18}O$ record with other dated natural records, such as ocean or lake sediments, geological records; flow modelling; dating with radioisotopes including ^{14}C, ^{36}Cl, ^{10}Be etc. and identifying world-wide and/or local, historical, natural and/or anthropogenic events, such as volcanic eruptions and typical nuclear bomb tests, are all widely used in ice core studies. Annual layer counting and known age horizon comparisons generally have higher precision, and quite often can achieve absolute age dating.

For ice cores recovered from low rate of accumulation areas, such as the Agassiz Ice Cap, annual layer counting can only be applied to a very limited depth because of wind scouring and diffusion of chemical elements within ice masses, which smooth out the

seasonal peaks (Johnsen, 1977; Fisher et al., 1983; Clausen and Langway, 1989). The identification of known age horizons, combined with other physical and chemical property measurements such as $\delta^{18}O$, ECM, summer melt layer counting and acid profiles, can be compared to Greenland ice core profiles (Fisher, 1983). The high accumulation rate on the Greenland Ice Sheet has allowed a detailed chronology to be established. However, the high resolution and speed with which ECM profiles are produced offer a time-depth relationship that can be established in the field during drilling.

The time scale for the first ice core drilled on the Agassiz Ice Cap, (Core A77), was first obtained by measuring chemistry and dust in 12 segments of core at resolutions of more than 6 samples per year so as to be able to see annual variations in dust, and positive ion chemistry as well as liquid chromatography (anions) and pH. Then the A77 ECM record was put on this time scale and compared to that for Dye 3 and Camp Century (Greenland). The 8 major ECM peaks for A77 were also the major ones for Greenland within the errors in the initial time scale (about 10%). Then the A77 time scale was adjusted to put the major ECM peaks at the Dye 3 dates. This procedure works for A77 back to about 7000 BP, after which the layer thicknesses are too small to take fine enough samples. The $\delta^{18}O$ "end of the ice age" transition was set to the Dye 3 age, which at that time was thought to have been 10,700 BP. All the other Agassiz cores were tied

into A77 using flow time scales adjusted so their ECM records best fitted the A77 major peaks. Hence all the Agassiz records are tied into Dye 3. However, the Dye 3 time scale in the early Holocene is thought to be wrong and the new summit GRIP/GISP2 age for the "transition" is 11,550 BP instead of 10,700 (Fisher et al., 1994). So the A93 ECM from the Agassiz Ice Cap is pinned at this new transition date. Details will be discussed in 3.1.2, Dating in A93 ice cores.

1.5 Definition of correlation coefficient

The correlation coefficient calculation is frequently used in this thesis in order to compare ECM records between cores, to estimate variability and to reduce noise from ECM records. Correlation is defined as the degree to which two variables are related. It can be calculated from the covariance which indicates if the variability of one variable is linked to the variability of another. Since each variable can have different units, it is preferable to normalize the covariance of two variables x and y by the product of their standard deviations σ_x and σ_y. The new parameter is the coefficient of correlation, ρ_{xy}. When the mean of the population is known, the coefficient of correlation is calculated as follows:

$$\rho_{x,y} = \frac{\sigma_{x,y}}{\sigma_x . \sigma_y}$$

in which, σ_{xy} is the population covariance; and σ_x^2 and σ_y^2 are the variances of x and y respectively. They are defined as follows:

$$\sigma_{x,y} = \frac{1}{N}\Sigma(x_i - \mu_x)(y_i - \mu_y)$$

$$\sigma_x^2 = \frac{1}{N}\Sigma(x_i - \mu_x)^2$$

$$\sigma_y^2 = \frac{1}{N}\Sigma(y_i - \mu_y)^2$$

where μ_x and μ_y are the known population means of variables x and y.

When the population means are not known, the sample's correlation coefficient, γ_{xy} can be estimated from:

$$\gamma_{x,y} = \frac{S_{x,y}}{S_x . S_y}$$

where S_{xy} is the sample covariance of x and y, S_x^2 and S_y^2 are the variances of x and y respectively; and

$$S_{x,y} = \frac{1}{n-1}\Sigma(x_i - x_{avg.})(y_i - y_{avg.})$$

$$S_x^2 = \frac{1}{n-1}\Sigma(x_i - x_{avg.})^2$$

$$S_y^2 = \frac{1}{n-1}\Sigma(y_i - y_{avg.})^2$$

The correlation coefficient, γ_{xy} varies from -1 to 1; with a value of zero indicating no correlation, and values of -1 and 1 indicating perfect negative or positive correlation, respectively. A negative correlation between 2 variables indicates that, on average, as one variable increases, the other decreases,

1.6 $\delta^{18}O$ definition

Many climate proxies can be used to deduce the palaeoclimate information. $\delta^{18}O$ is one that is most widely used due to its reliability even though its analysis is time consuming. $\delta^{18}O$ is defined as:

$$\delta^{18}O = \frac{(^{18}O/^{16}O)_{sample} - (^{18}O/^{16}O)_{SMOW}}{(^{18}O/^{16}O)_{SMOW}} * 1000‰$$

Air temperature at the time of vapour condensation is the major factor affecting $\delta^{18}O$ even though other factors such as, vapour source, altitude and seasonal distribution of

snowfall can be important. Fisher and Koerner (1979) calculated and concluded that the later factors had only negligible effects on $\delta^{18}O$ of ice cores from Devon Ice Cap. Therefore, $\delta^{18}O$ records can directly be considered as a temperature proxy.

1.7. Collaboration

This work is part of a collaborative project examining ice core from the Canadian Arctic. David A. Fisher, Mike Gerasimoff, John Brennan and John Sekerka in the National Resources of Canada (NRCan in short) drilled the A93.1 and A93.2 ice cores. David Fisher also did the precision ice core dating and involved in the data analysis and figure preparation. Roy M. Koerner from NRCan coordinated the field program. Akira Kudo from the National Research Council of Canada (NRC in short) designed the independent and flexible ECM electrodes. Ian D. Clark from the University of Ottawa contributed his ideas and suggested the writing strategy of this thesis. Erik W. Blake from the Icefield Instruments Inc. cut the whole A93.1 ice core to create a microtome smoothed surface on site and did the fourth ECM (three sections of the fourth ECM is included in this thesis). Van Luong from NRC designed the controlling electrics and data collecting program of the ECM system. John Woods from NRC analysed 154 samples for the major anions in a 3 metre long ice core. I, myself, built, tested, modified and calibrated the ECM system. During the field trip,

I assisted in the ice core drilling and handling, and carried out three ECM profiles on site from A93.1 and A93.2 ice cores respectively. After the field trip, I did all the data processing, including primary data analysis, validation and criteria determination for ECM data in connection with different ice core sections. This included simple and moving averages in different scales, coarse ice core dating, correlation coefficient analysis and figure preparation with David Fisher's help and suggestion. The data capture and processing tasks represent the major component of this thesis.

2. Measurement theory and technology

2.1 Theory of ECM Signals:

Ohm's law gives that the direct current, I, flowing in an electrical circuit is directly proportional to the voltage, U, applied to the circuit and reversely proportional to the total resistance, R_t, of the circuit:

$$I = \frac{U}{R}$$

where I has a unit of ampere(A), U with units of volt(V) and R with units of ohms (Ω). The resistance is the reciprocal of the conductivity, ρ, of the circuit, that is

$$R = \frac{1}{\rho}$$

Pure ice has low electrical conductivity, giving only $\sim 10^{-8}$ A current when applying $\sim 10^{3}$ V/cm voltage gradient on it at temperature ranges of 0 to -60°C for high purity ice crystal (water purity of 18 MΩ/cm)(Camp et al., 1967). When applying a voltage to an ice crystal at a single position, the current changes with time dramatically as shown in Figure 2a. The curve of current change with time can be grouped into three stages. The first stage; from t_0 to t_1, where the current does not change essentially; the

second; from t_1 to t_2, is the dramatic variation in conductivity and the third; after t_2, is the stable stage. Experiments by Maidique et al. (1971) and Hammer (1980) explained the three stages. The initial stage, usually lasting for 0.1 to 0.5 seconds, is the onset region of the space-charge pile-up, i.e. the mobile extrinsic charge carriers are available in the ice crystal where the activation energy is zero. Therefore, the current, I, in this stage is constant. The second stage, usually a few seconds, is the process of space charge pile-up in which the field strength at the cathode rises gradually. In the third stage, field emission sets in, which produces an almost constant current. The stable (flat) portion of both the first and third stages can be used for ice conductivity measurements. However, electrical conductivity measurements on the third stage is not practical because a long period of time is needed to achieve stability. It is only the first stage, where the current does not essentially change with time either, that is suitable for the ice crystal conductivity measurement. Hammer (1980) found that the application of an electrical field on an apparently homogeneous piece of ice could change the electrical properties of the ice up to 2.5 mm around the electrodes. There was, however, no significant change beyond this. Therefore, it is feasible to measure the ice electrical conductivity if the ice has a clean surface with a thickness and width larger than 2.5 mm, and contact time for any 2.5 mm region is less than 0.1 seconds (i.e. 25 mm/s movement rate) (Refer Figure 2b and Section 2.2).

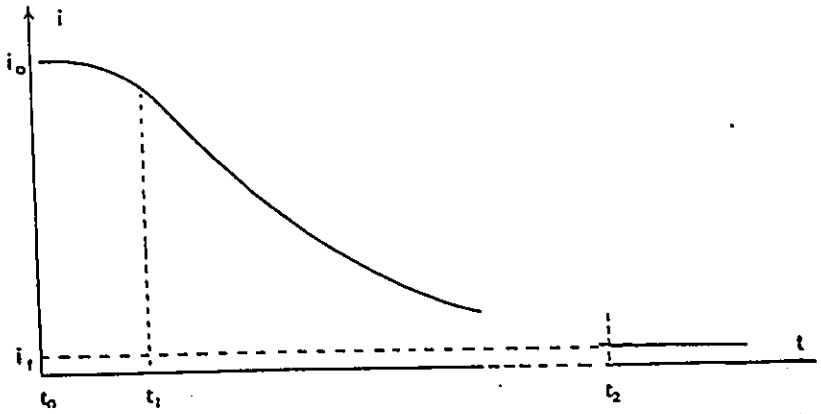

Figure 2a. Current change with time after applying an electrical field on ice at a fixed position (After Hammer, 1980).

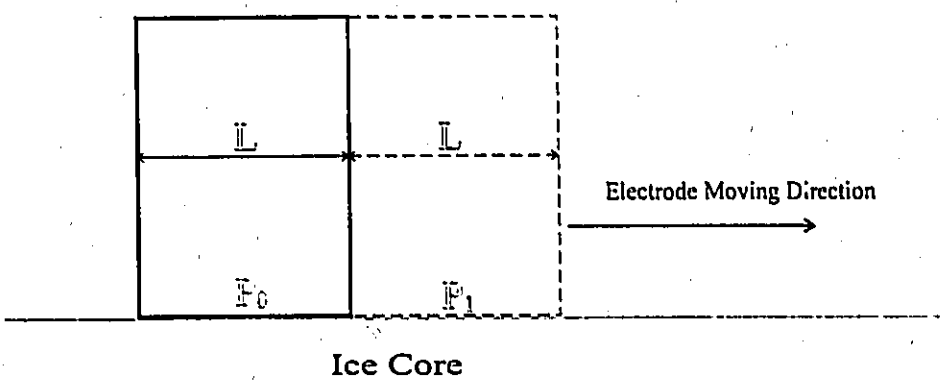

Figure 2b. Sketch of the minimum electrode speed. Electrode speed must be equivalent to or larger than the ratio of the electrode's tip width and t. Here, L is the width of electrodes tip; P_0 and P_1, the position of electrodes at t_0 and t_1. Therefore, the wider the electrode's tip width, the lower the ECM resolution will be theoretically.

2.2 Description of the electrical conductivity measurement system:

As shown in Figure 3a, the ECM device consists of four elements: (1) high voltage power supply, (2) travelling electrodes, (3) signal sampling and (4) data collection system. The high voltage power supply is a Model TC951 from TENNELEC Limited. It can supply DC voltage ranging from 0 to 3000 V. The electrodes and their travelling rail were manufactured as part of this project at the National Research Council of Canada (NRC). The electrodes are independently adjustable and flexible with constant distance between them. They have been designed in this manner in order to achieve a better contact between the electrodes and the ice core surface (See Figure 3b). The travelling rail is made of highly polished aluminium. The electrodes travel smoothly when the temperature is higher than -25°C but there was some distortion when the temperature was lower than -30°C. The signal sampling resistor is a standard resistor box, (Decade Resistance Box Type 602m, General Radio Co.), which has been highly shielded and with a very low temperature instability (Instability between room temperature and -12°C is less than 0.01 Ω).

A computer code "Icecore" II was compiled in Pascal for data collection and system control. Based on the previous discussion, the electrode travelling speed along the rail

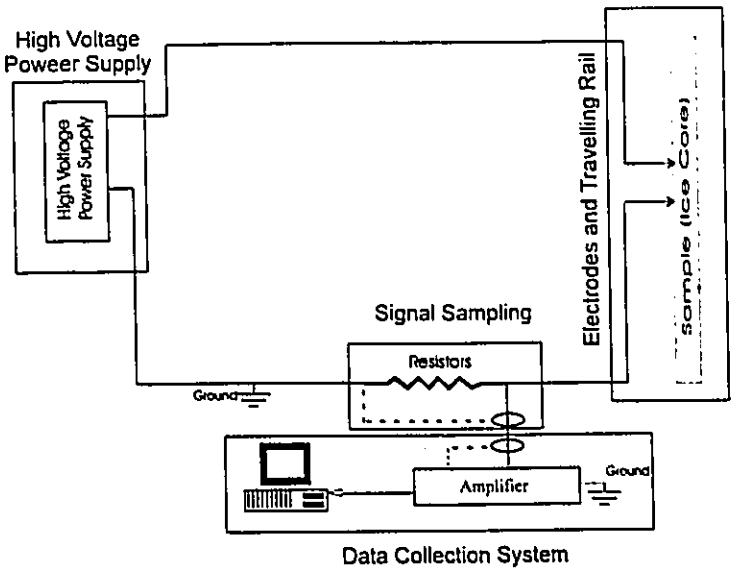

Figure 3a. Diagram of four component ECM system.

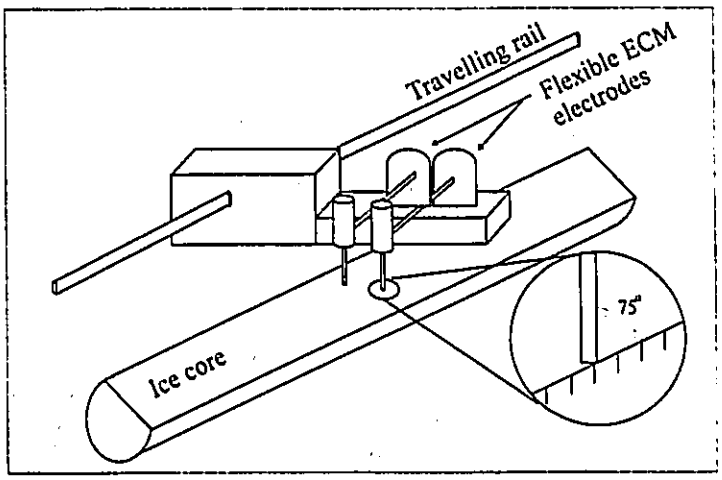

Figure 3b. Sketch of flexible ECM electrodes and travelling rail. The angle between the electrodes and the ice core surface is about 75° in order to achieve a better resolution. The two electrodes are independent.

should be equal to or larger than the ratio of the electrode's width and t_1 (0.1 to 0.5 seconds) so that a high resolution can be achieved (Figure 2b). As shown in Figure 2b, assume L is the width of the electrode tip. For a resolution equal to the tip width to be achieved, the electrodes have to travel from P_0 to at least P_1 within t_1 (0.1-0.5 second). The ECM signal measured at P_0 will be the combination of the ice core covered by the electrode tip width, L. Theoretically, the smaller the electrode tip is, the higher the resolution will be if the electrodes can travel the distance of the tip width within the time range of t_1. To ensure this, a value of t_1=0.1 second was taken to calculate the electrode travelling speed. Two factors were taken into consideration for the electrode's tip width: its rigidness and its contact surface with the ice core. The electrodes were made of a ϕ=3 mm diameter stainless steel bar which had been sharpened on both sides. The real contact width of the electrodes and the ice core is about 1 mm when an angle of about 75 degrees (Refer to Figure 3b) is introduced between the electrodes and the ice core surface even though the electrode tip width is about 3 mm. Therefore, the electrode travelling speed was set at 20 mm per second or larger, which was higher than $V = L/t_1$ = 1 mm/0.1 second = 10 mm/second. The electrodes were set two centimetres apart in order to avoid overheating the ice cores between the electrodes.

2.3 Voltage Stability and Device Response Testing

Even though changes in an applied voltage does not change the ECM trend (shape), it does change ECM amplitude (Taylor, 1992). There may be little difference in ECM on a single ice core section when the applied voltage varies a little bit. However, a problem may result when ECM are required for the full ice core, which may extend to hundreds or even thousands of metres long and when the ice core includes different historical climate periods. The DC high voltage power supply used in the device has a maximum current output of 3 mA. Rough measurements of ice cores showed the ice core resistance was higher than $10^8\ \Omega$. Based on this, the possible maximum current under 1500 V is less than 0.015 mA, which is only about 0.5% of the power supply's limit. Therefore, it is assumed the voltage supply is stable in this load range, providing a stable power supply (See Figures 4a and b).

The maximum voltage input of the data collection system was 0.7 volts. Therefore, the signal sampling resistor was set at 40,000 Ω in order to avoid overflow. This resulted in a maximum of 0.6 volt input into the data collection system when ice core resistance between the two centimetre apart electrodes reaches 10^8 ohms. Two tests were carried

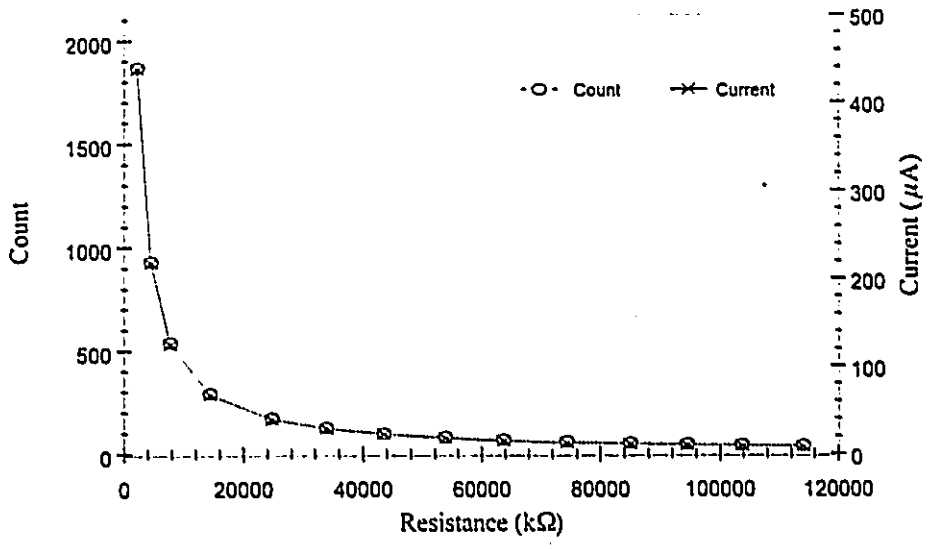

Figure 4a. Device response to different loads under 979 V and 10 kΩ sampling resistance.

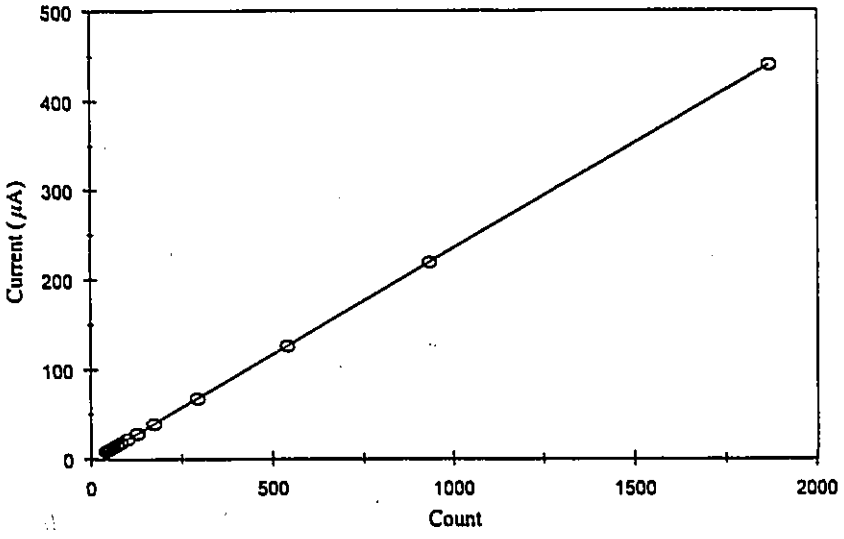

Figure 4b. Linearity of current change with counts (with 10 times amplification).

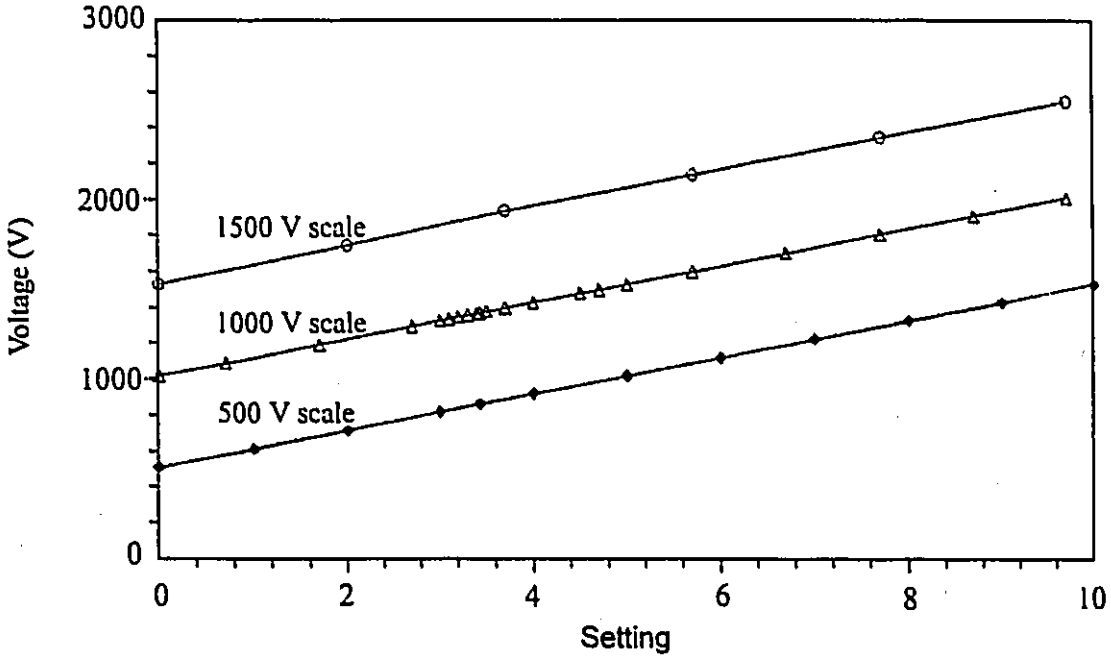

Figure 5. DC power supply linearity at different scales and settings.

out for voltage stability and device response. The results for voltage test are shown in Table 2 and Figure 5. All three scales have high linearities at different settings within the various voltage ranges. For convenience, 3000 V scale and setting at 4.7 was selected to supply a 1500 V DC power supply. For the device response test, 979 V and 10.000 Ω signal sampling resistor were used, instead of 1500 V and 40.000 Ω. The reason for this change is that no suitable high value resistors were available at the time.

The whole system should obey Ohm's law if each component is ohmic. If the whole system follows Ohm's law, the device response should linearly reflect the current calculated from the applied voltage and the total circuit resistance in the system. The results showed in Table 3 and Figures 4a and b, demonstrate that the whole system is ohmic and has a high linear response to the system current with a correlation coefficient of 0.999998 and conversion equation of

$$\text{Current } (\mu A) = \frac{\text{Count} - 5.768}{4.234}.$$

where the Count is the quantized (digitized) signal picked up by the computer; 4.234 is the converting factor between counts and current; the constant of 5.768 is specific to the system (See next section).

Table 2. ECM power supply linearity testing and the result linear regression.

Scale	Setting	Voltage	Scale	Setting	Voltage	Scale	Setting	Voltage	Scale	Setting	Voltage
500	0	511	1000	0	1021	1500	0	1531	2000	0	2040
	1	613		0.7	1091		2	1735		2	2240
	2	716		1.7	1194		3.43	1882		3.43	2390
	3	819		2.7	1297		4	1940		4	2450
	3.43	863		3.43	1372		6	2140		6	2650
	4	921		3	1328		8	2350			
	5	1021		3.1	1338		10	2550			
	6	1122		3.2	1349						
	7	1225		3.3	1359						
	8	1328		3.4	1369						
	9	1430		3.5	1380						
	10	1530		3.7	1399						
				3.7	1400						
				4	1430						
				4.5	1481						
				4.7	1500						
				5	1530						
				5.7	1600						
				6.7	1703						
				7.7	1807						
				8.7	1909						
				9.7	2010						
				4.7	1500						

Regression output:

500 scale

Constant		512.05
Std Err of Y Est		1.1119
R Squared		1.0000
No. of Observations		12
Degrees of Freedom		10
X Coefficient(s)	101.91	
Std Err of Coef.	0.105	

1000 scale

Constant		1021.68
Std Err of Y Est		1.1346
R Squared		1.0000
No. of Observations		23
Degrees of Freedom		21
X Coefficient(s)	101.92	
Std Err of Coef.	0.105	

1500 scale

Constant		1531.26
Std Err of Y Est		2.0534
R Squared		1.0000
No. of Observations		7
Degrees of Freedom		5
X Coefficient(s)	101.98	
Std Err of Coef.	0.242	

2000 scale

Constant		2039.17
Std Err of Y Est		2.6478
R Squared		0.9999
No. of Observations		5
Degrees of Freedom		3
X Coefficient(s)	102.02	
Std Err of Coef.	0.590	

Table 3. ECM device quantized (digitized) signal (count) response to different resistance settings and the calculated current based on Ohm's law to set up the relationship between count and current.

Total resistance (kΩ)	114074	103794	94534	84964	74364	63764	53774
Calculated current (μA)	8.58	9.43	10.36	11.52	13.16	15.35	18.21
Device response (count)	42.13	45.68	49.58	54.33	61.64	70.76	82.66
Total resistance (kΩ)	43494	33864	24744	14454	7774	4474	2224
Calculated current (μA)	22.51	28.91	39.57	67.73	125.93	218.82	440.20
Device response (count)	100.44	127.82	173.43	293.30	541.25	932.42	1870.50

2.4 ECM Device Background (Noise)

The ECM device background is defined as the signal collected by the data collecting system when the load is zero (open distance in the air) between the two electrodes under the experimental conditions of 1500 V applying voltage, 40 kΩ sampling resistance, 2 cm apart electrode spacing and 2 cm/s electrode travelling speed.

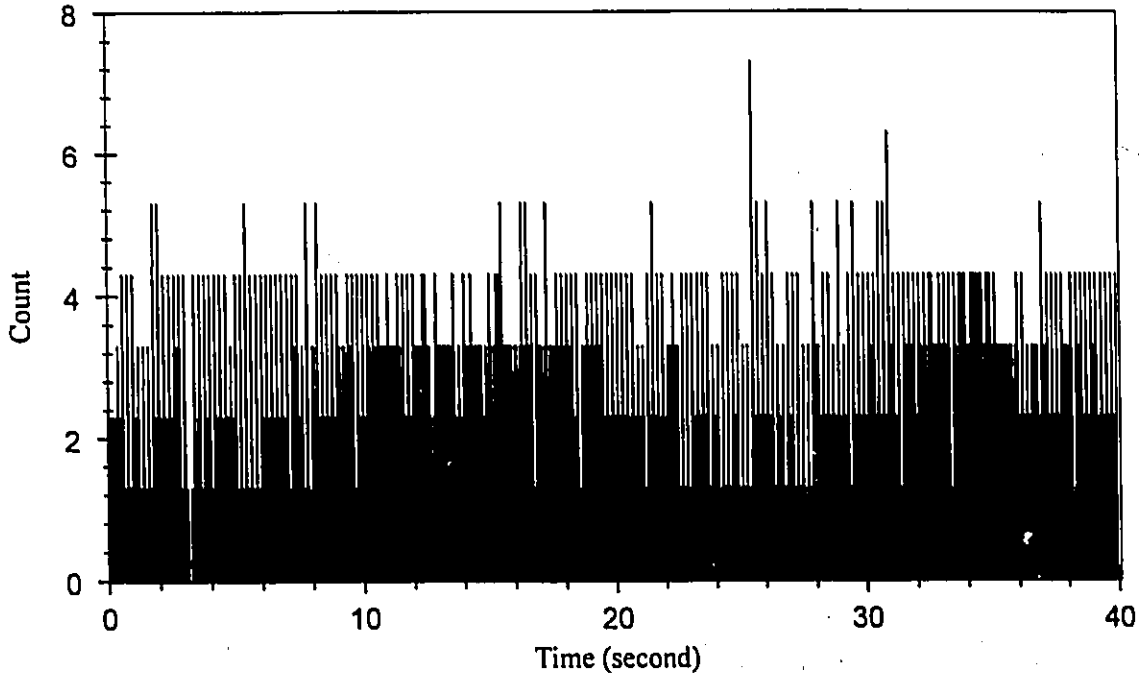

Figure 6. Device response background under 1,500 volts and 40 k-ohm sampling resistance.

The background is shown in Figure 6. A total of 1000 data sets were collected. It seems that a maximum of 7 counts of background is typical (See equation in previous section also). The noise is probably from the electronics of the system components.

2.5 Details of Field Measurements:

The drilling for the two 1993 ice cores commenced on May 1st and ended on May 15th with a three day storm interruption (from May 11th to 13th). Both ice cores 93.1, (123.35 metres to bed rock), and 93.2 (121.51 metres to near bed rock), were drilled with an electro-mechanical drill that obtains 8.4 cm diameter cores about 1 m in length. The core recovery is over 98% and the core quality is generally very good with no obvious contamination in terms of electrical conductivity. Core A93.1 has total of 430 sections in its 121.7 metre long ice core obtained, resulting in an average section length of 0.283 metre while Core A93.2 has total of 223 sections in its 101.0 metre long ice core obtained, resulting in an average section length of 0.453 metre. Therefore, Core A93.2 quality is better than Core A93.1. The drilling sites for the two ice cores were two metres apart at 81°49.9' N and 71°55.07' W and very near the Agassiz Ice Cap dome (See Figure 1).

Two ECM systems were used in the field, one from NRC and the other from Ice Field Instrument Ltd (IFI). Both ECM systems were operated in an ice pit, measuring about 5 m(L) x 2.5 m(W) x 2 m(H). The temperature in the pit ranged from -10.5 to -24.0 °C and varied mainly between -14 and -18 °C. The average of 368 temperature readings during ECM of Core 93.1 (both cut and uncut) was -19.3°C and the temperature average for Core 93.2 (uncut only) was -12.43 °C from 152 readings. The moving speed of ECM electrodes was 2.85 cm/s for NRC system (sampling rate was mainly 25 samples per second with exception of 16.7 samples per second when ice core length was longer than one metre) and the applied DC voltage was 1500 V with an electrode distance of 2.0 cm. ECM data were collected on an IBM compatible 386 lap-top computer and processed after the field work.

ECM were first carried out on the original surface of the freshly recovered ice core, right after stratigraphic examination. After the first ECM was done, a band saw and a microtome knife were used to create a flat and smooth surface on the ice core, followed by two measurements of the two ECM systems respectively. The electrode tracks on prepared smooth surface may not travel right on the same surface position as the first ECM was carried out and the two ECM measurements by the two different ECM systems may also not be on exactly the same electrode tracks either. The time difference of ECM

runs on the original and microtome knife prepared surfaces of Ice Core 93.1 was about 40 minutes. The IFI ECM system has a very similar design to the NRC one; as were the operation conditions. The time difference between the measurements of the two ECM systems was less than 10 minutes.

2.6 Validation of ECM results by major anion analysis:

Acids in ice cores are those which can easily give hydrogen ions, such H_2SO_4, HNO_3 and HCl. HF is also a strong electrolyte but relatively less abundant comparing with those. Anions mean all the ions with negative sign, such as those SO_4^{2-}, NO^-, and Cl^-. Strong acids ionize into ions, anion and cation

$$H_iX_j = H^+ + H_{i-1}X_j^-$$

and further

$$H_{i-1}X_j^- = H^+ + H_{i-2}X_j^{2-}$$

Meanwhile, salts also ionize into anions and cations

$$M_iX_j = M^{\nu+} + M_{i-1}X_j^{\nu-}$$

where ν is the valence property of the cation.

Therefore, the measurement of total anions is a measurement of a combination of anions from both acids and salts with same anion element. H^+ is the dominant cation in Holocene glacier ice (Clausen, 1989), and H^+, SO_4^{2-}, NO^- and Cl^- have closely associated relation in glacier chemistry. H^+ concentration level is determined mainly by the amount of H_2SO_4, HNO_3 and HCl present. In other words, SO_4^{2-}, NO_3^- and Cl^- are the dominant anions. Therefore, variation of total major anion concentrations is roughly corresponding to the variation of H^+ concentration.

ECM are measurements of total electrical charge conducting elements in the ice core under the conditions applied. To examine the effectiveness of ECM in reflecting the ion strength of the ice core, three sections of ice core 93.2, a total of 308 cm in length, were analysed for major anions, NO_3^-, SO_4^{-2} and Cl^-. Results are shown in Figure 7. ECM were carried out on fresh surfaces immediately before anion analysis sampling. Anion samples were taken every 2 cm after washing away the contaminated surface. The samples were melted in sealed sample bags and later analysed with a Waters Ion Chromatography analyser.

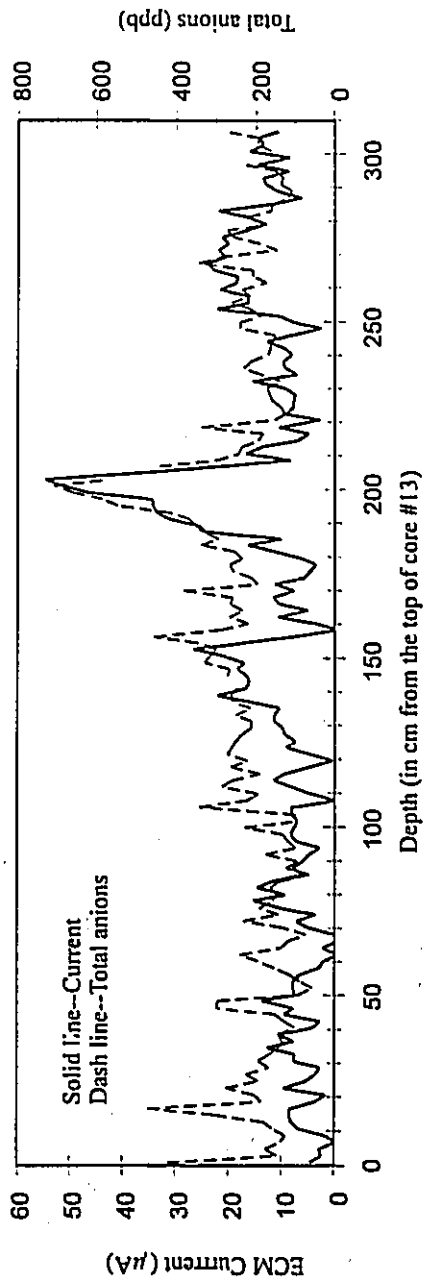

Figure 7. Validation of ECM results by anion analysis on A93.1 ice core #13-15.

In order to compare ECM data with anion data, the ECM data were averaged on two centimetre intervals. The two sets of data, which are measures of two totally different variables, show a strong correlation coefficient of 0.674 (Figure 7) and have a quite similar trend. In particular, the largest peak, located 200 cm from the top of Core #13, appears at the exact same position. The strong correlation validates the effectiveness of the ECM device even though the details of the two data sets do not fully match each other. This may have partly resulted from a low sampling rate and lack of other minor conductivity components data, such as F^- and partly due to the fact that ECM reflects the sum of acids but sum of anions.

3. Data and Discussion

3.1 Establishment of Age-Depth Relationship:

ECM is fundamentally a measure of components which can conduct electrical charges, of which acids are the major contributors. Volcanic events produce large amounts of volcanic gases, such as SO_2 which oxidizes and combines with water to form sulphuric acid (Shaw, 1989). Fall-out from moderate volcanic events are local in influence, but larger, more violent volcanic events can eject volcanic dust and gases far into the stratosphere, where they may be spread globally and re-enter into the troposphere up to two to three years after the eruption (Legrand, 1987). The volcanic aerosols and dust in the troposphere then settle with precipitation on the ground. Gases are oxidized and dissolved in precipitation. Therefore, worldwide volcanic events should be recorded in glaciers. If these powerful eruptions are dated in the geological or historical record, they can be used as bench-markers for ice core dating (Hammer, 1985; Langway et al., 1988; Clausen and Hammer, 1988; Hammer, 1989).

Volcanic eruptions in the past 500 hundred years are well recorded (Lamb,1970; Bradley and Jones, 1992). Signals of volcanic events like Katmai (Alaska, AD 1912),

Tambora (Indonesia, AD 1815), Laki (Iceland, AD 1873) and some events older than 500 years have clearly been recognized in Greenland and Arctic ice cores. The Eldgja eruption (Iceland, AD 934), Mazama (N.W. U.S., 4,400 BC) and unknown events in AD 1259 (unknown, in Dye 3) and 50 BC (unknown, in Dye 3) have been found in ice cores recovered from Greenland and Canadian High Arctic ice caps (Fisher and Koerner, 1988; Thomas et al.,1993).

Climatic events, such as the transition from Wisconsin to Holocene at about 11,550 BP (Johnsen et al., 1992), matched by a large $\delta^{18}O$ shift in glacier ice, provide an additional time marker for ECM record dating controls. Also, as the Agassiz bottom ice is probably no older than the late Sangamon Interglacial there is a rough lower boundary for the chronology (Koerner, 1989). Theoretical flow modelling together with these time horizons have been used for age-depth control in the Agassiz Ice Core studies since 1977 (Dansgaard and Johnsen, 1969; Fisher et al., 1983; Fisher and Koerner, 1988; Fisher et al., 1995). Throughout this thesis, ages are referred to in calendar years before present, which is the year of drilling, otherwise the year AD 2000 as noted in the figures.

3.1.1 ECM signal and chronology in A84:

For the A84 ice core dating, the initial theoretical time scales were "tuned" using volcanic acid layer stratigraphy. The acid stratigraphy detected using the ECM method was assigned a chronology using known historical records or the dates given from the Dye-3 ice core (Langway et al., 1988; Hammer 1984). Table 4 gives the volcanic stratigraphy for A84 and A93.1. Figure 8a gives 5 centimetre averages of the ECM data for core A84 and A93.1 (from prepared surface), and the major events are noted. For individual volcanic acid layers the maximum peak heights are much higher than the 5 centimetre averages. $\delta^{18}O$ and summer melt percentage for A84 are also shown in Figure 8a. The summer melt percentage (PC) is defined as:

$$PC = \frac{\text{Annual melt}}{\text{Annual accumulation}}$$

where the melt and accumulation are both in ice equivalent.

Similar peaks and minima can also be cross-correlated between earlier Agassiz cores (Fisher an Koerner, 1994; Fisher et al., 1995). Figures 8b and 9 show that the ECM

Table 4. The A84 and A93.1 time scales.

Depth (real) (m)		Depth (ice) (m)		Age		Volcanic event or marker
A84	A93.1	A84	A93.1	(AD)	(BP)	
15.16		8.18		1912	81	Katmai
18.50		10.78		1884	109	Krakatoa
26.43		17.00		1816	177	Tambora
29.73	29.00	19.65	19.059	1783	210	Laki
34.70	34.15	23.81	23.342	1715	278	ECM minimum (in Dye 3)*
35.71		24.68		1695	298	Unknown (in Dye 3)*
39.74		28.23		1642	351	Komagatake
43.87		31.96		1561	432	ECM minimum (in Dye 3)*
48.22	46.50	35.97	34.372	1462	531	Unknown (in Dye 3)*
48.66	47.00	36.37	34.834	1455	538	Unknown (in Dye 3)*
50.99		38.55		1413	580	Unknown (in Dye 3)*
57.68	55.40	44.80	42.666	1259	734	Unknown (in Dye 3)*
58.63		45.69		1229	764	Unknown (in Dye 3)*
68.85	64.70	55.21	51.348	934	1059	Eldgja
84.69		69.94		-50	2043	Unknown (in Dye 3)*
104.15		88.30		-3150	5143	Unknown (in Dye 3)*
108.48	97.65	92.38	82.148	-4400	6393	Mazama
115.44	108.20	98.92	92.115	-9557	11550	δ transition age (Johnsen et al., 1992)

* Dye 3 ages come from (Hammer 1984).

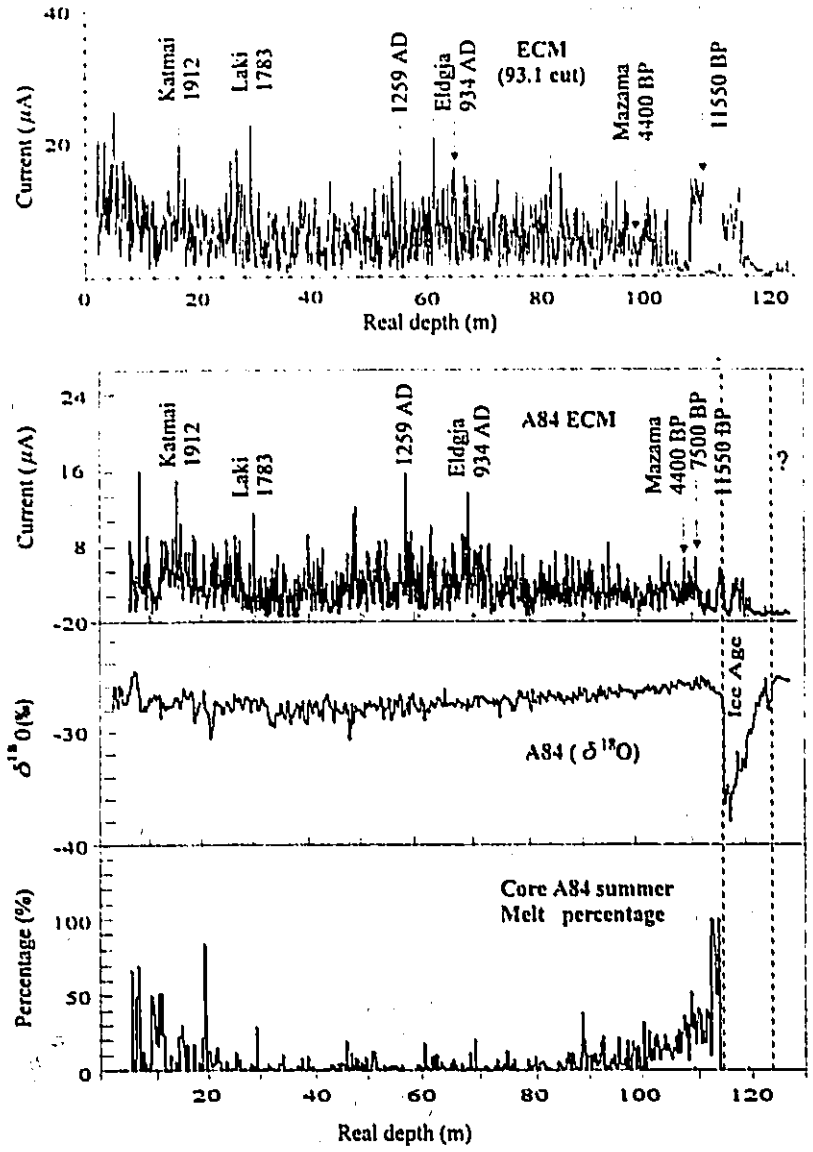

Figure 8a. Comparisons between ECM, $\delta^{18}O$ and summer melt of A84 core and ECM of A93.1. A84 ECM current is calculated from the original voltage series by dividing the resistance of 38,500 ohms. Major volcanic events are marked in the figure and compiled in Table 4. Major features between A93.1 and A84 cores are well matched (Modified from Zheng et al., 1995).

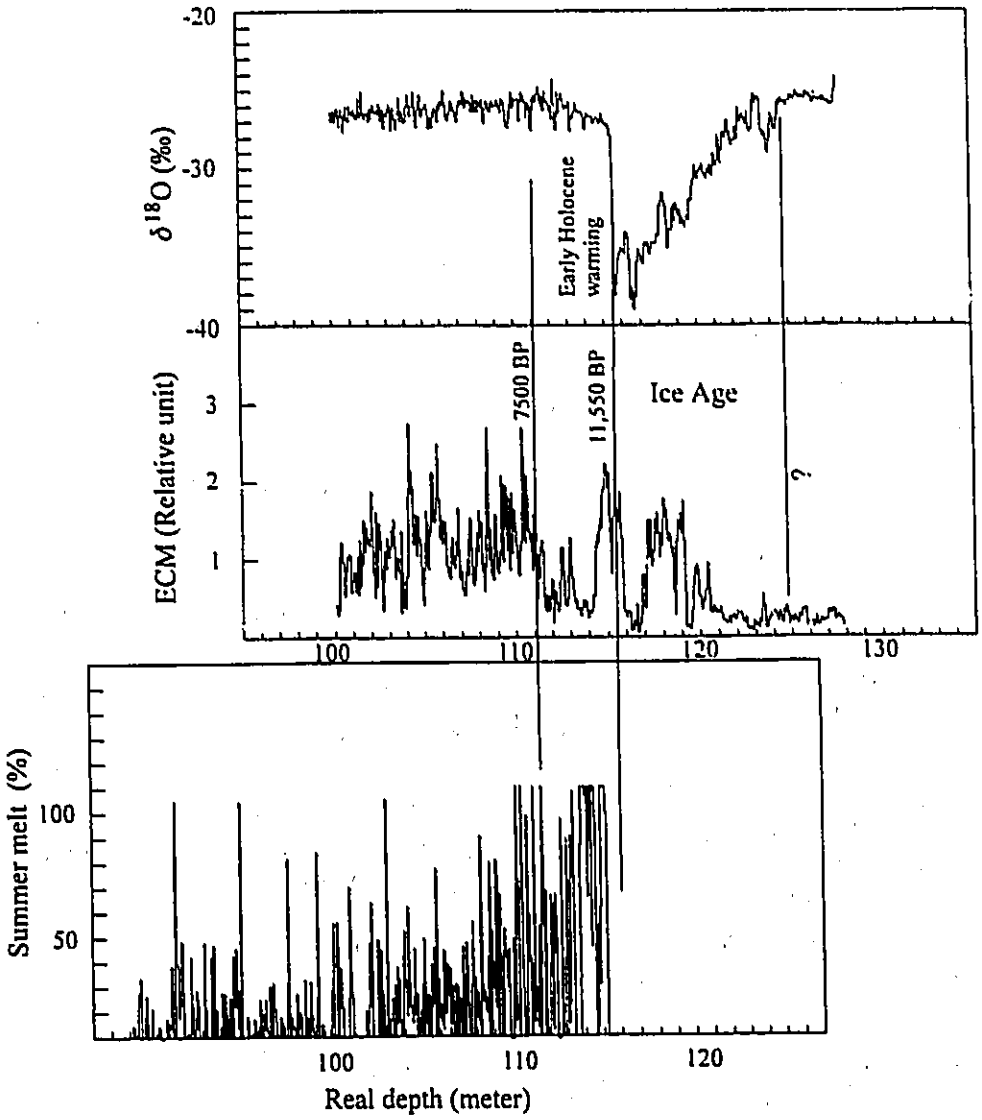

Figure 8b. Early Holocene and pre-Holocene ECM, summer melt and $\delta^{18}O$ records of core A84 (After Zheng et al., 1995).

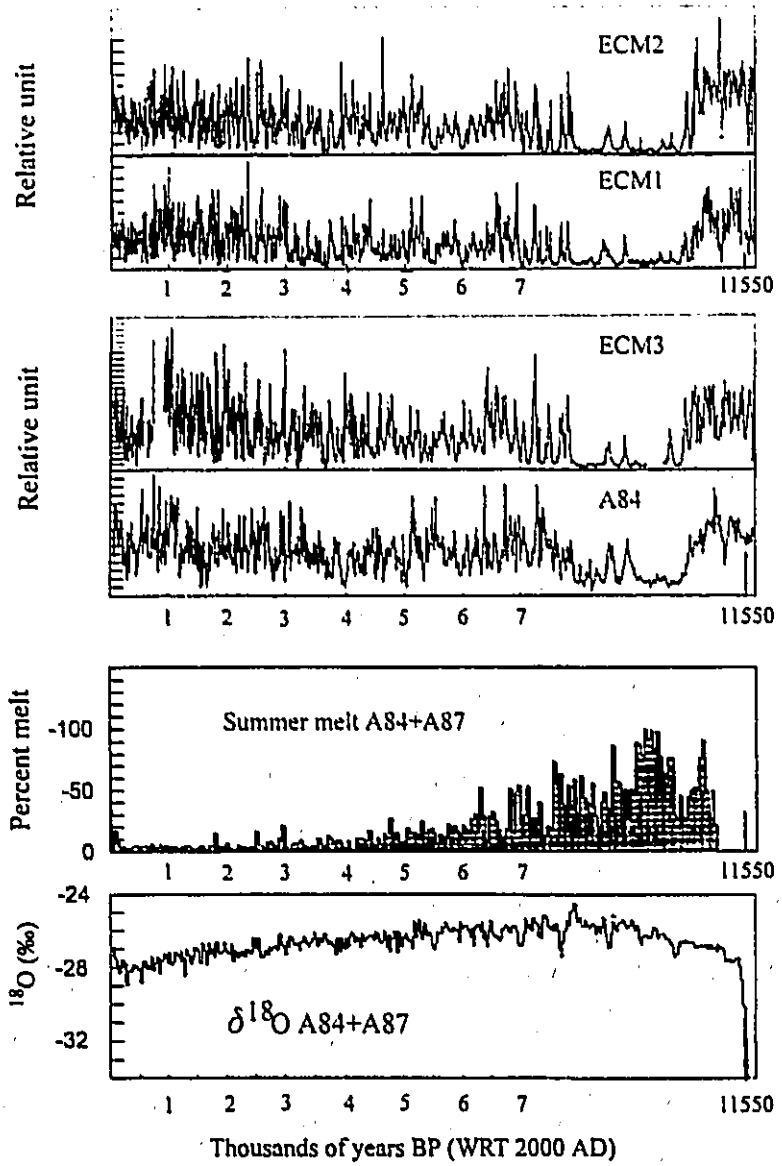

Figure 9. Comparison of 4 ECMs from A93 and A84 with summer melt and $\delta^{18}O$ results (Modified from Zheng et al., 1995).

signal is greatly reduced between about 7800 BP and about 10,500 BP. This 'low' ECM period is common to all the Agassiz cores and coincides with the period of extreme summer melt in the early Holocene (Figures 8 and 9) (Fisher et al., 1995; Zheng et al., 1995). Figure 9 shows the 5 year averages for ECM1, ECM2, ECM3 and ECM A84 for the Holocene. The time series were made using the one cm resolution data, which is adequate for such temporal resolution for the most recent 7000 years of the Holocene (See the bar at the bottom of Figure 12). Also shown in Figure 9 is the correlation optimized average melt layer percent and $\delta^{18}O$ time series made by adding the A84 and A87 series together to reduce noise (Fisher et al., 1995). The time scale is only defined back to about 7000 BP and again at the sharp $\delta^{18}O$ transition at the end of the Ice Age, which is assigned the GRIP/GISP2 age of 11,550 years BP, defined by the sharp $\delta^{18}O$ change.

The transition from Ice Age to Holocene, as defined by the large sudden enrichment in ^{18}O, is given the calendar age of 11,550 years BP (Johnsen et al., 1992). This date from the Summit ice core is still preliminary but is in good agreement with U/Th ages for the termination of the Younger Dryas (Bard et al., 1990). The A84 $\delta^{18}O$ profile is also included in Figures 8a and b, from which some of the major Pleistocene periods have been interpreted (Fisher and Koerner, 1986; Fisher, 1987; Koerner, 1989).

3.1.2 Dating in A93 ice cores:

A modified A84 time scale was initially used for A93 cores and later calibrated using the major ECM (volcanic) peaks (Table 4) that have been correlated with the A84 and A93 stratigraphies. Also, the timing of the $\delta^{18}O$ transition marking the termination of the last ice age is given the GRIP age of 11,550 years BP (Johnsen et al., 1992; Alley et al., 1993). As shown in Figures 8a, 9 and 11a, major features between A93 and A84 cores are well matched. Figures 10a and 10b show the Holocene time scales for A93 and A84 respectively. Ages between the 'known' fixed points are calculated (tuned) using a glaciologically correct interpolator (Fisher, 1978). Figures 10a and b show age versus ice equivalent depths that are calculated from the real measured depths using the measured density curve that is presented in Figure 10c.

For quick translation of depth into age during data analysis, an exponential-term modified polynomial equation was also developed as a reference. The equation was based on the bench markers listed in Table 4 plus surface age at 1992, ice core starting age (1.9 metre from surface) at 1986, and the end of the ice age at about 120,000 year BP (Fisher, 1987; Fisher and Koerner, 1988; Koerner, 1989). Pure multinominal fitting was first used for this purpose. However, it was hard to achieve a good fit in the last part

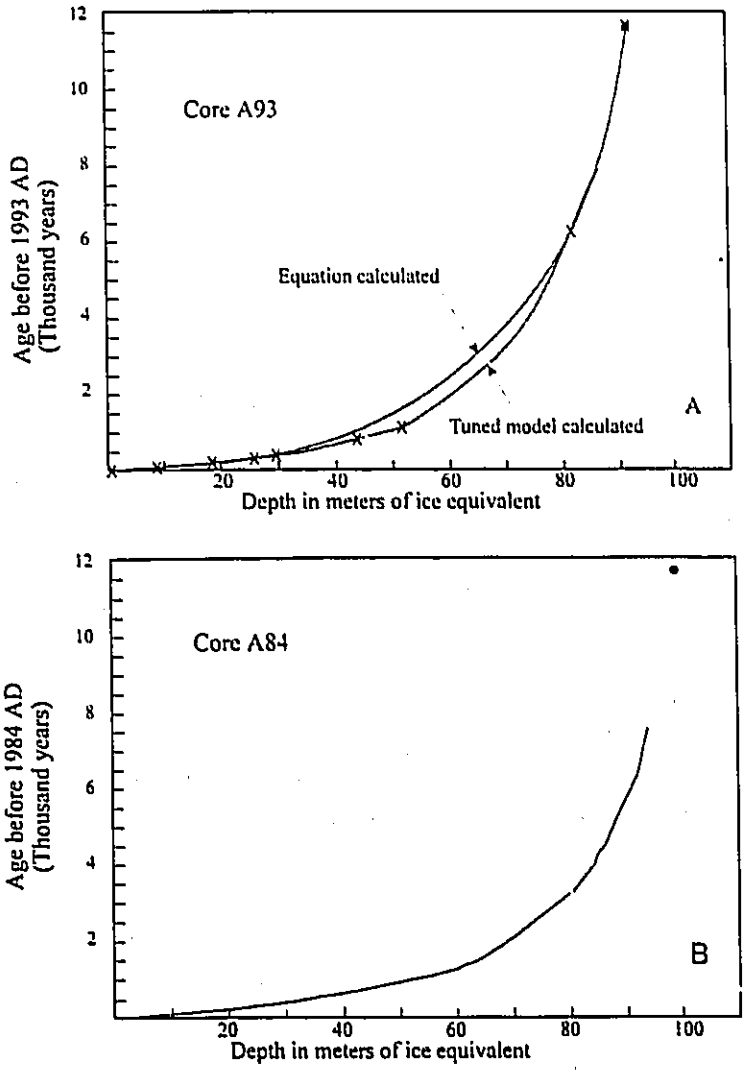

Figure 10a and b. Time scales for Ice Cores of A93.2 and A84 from the Agassiz Ice Cap of Canadian High Arctic. The 'known' fixed points are listed in Table 4. Ages between the fixed points are calculated (tuned) using a glaciologically correct interpolator (Fisher, 1978). The bench markers used for the modified multinomial function are also marked in Figure 10a with x (Modified from Zheng et al., 1995).

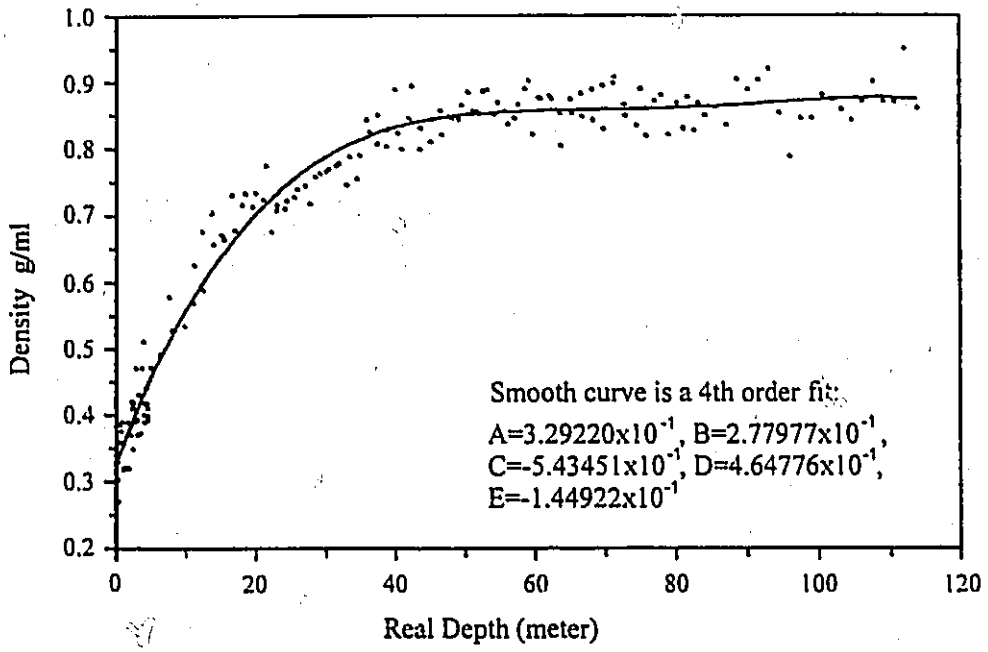

Figure 10c. Agassiz ice density change with depth (data for A84, A79 and A93)(After Zheng et al., 1995).

(about 30 metres) of the ice core because of the abrupt thinning of the annual ice thickness. One exponential term has been introduced in order to get a better fit of the whole ice core with the benchmarks. The two numbers in the exponential term were decided by trial and error. The function describing the age-depth relationship is plotted in Figure 10a with these bench markers marked by cross (x). The final fitting equation is as follows.

$$\text{Age(year BP)} = -17.5 + 11.995 \times \text{Depth} - 0.485 \times \text{Depth}^2 + 0.01227 \times \text{Depth}^3 - 0.0000253 \times \text{Depth}^4 + 0.00194^{(\text{Depth}/(\text{Depth}-190))}.$$

Both age-depth relationships show that annual ice layer thicknesses, about 12 cm ice equivalent at the surface of the ice core, gradually reduced to less than one millimetre at the transition area from Wisconsin to Holocene, without a sudden change. The average annual thickness in pre-Holocene ice is 0.12 millimetres assuming the bottom ice has an age of 120,000 year BP.

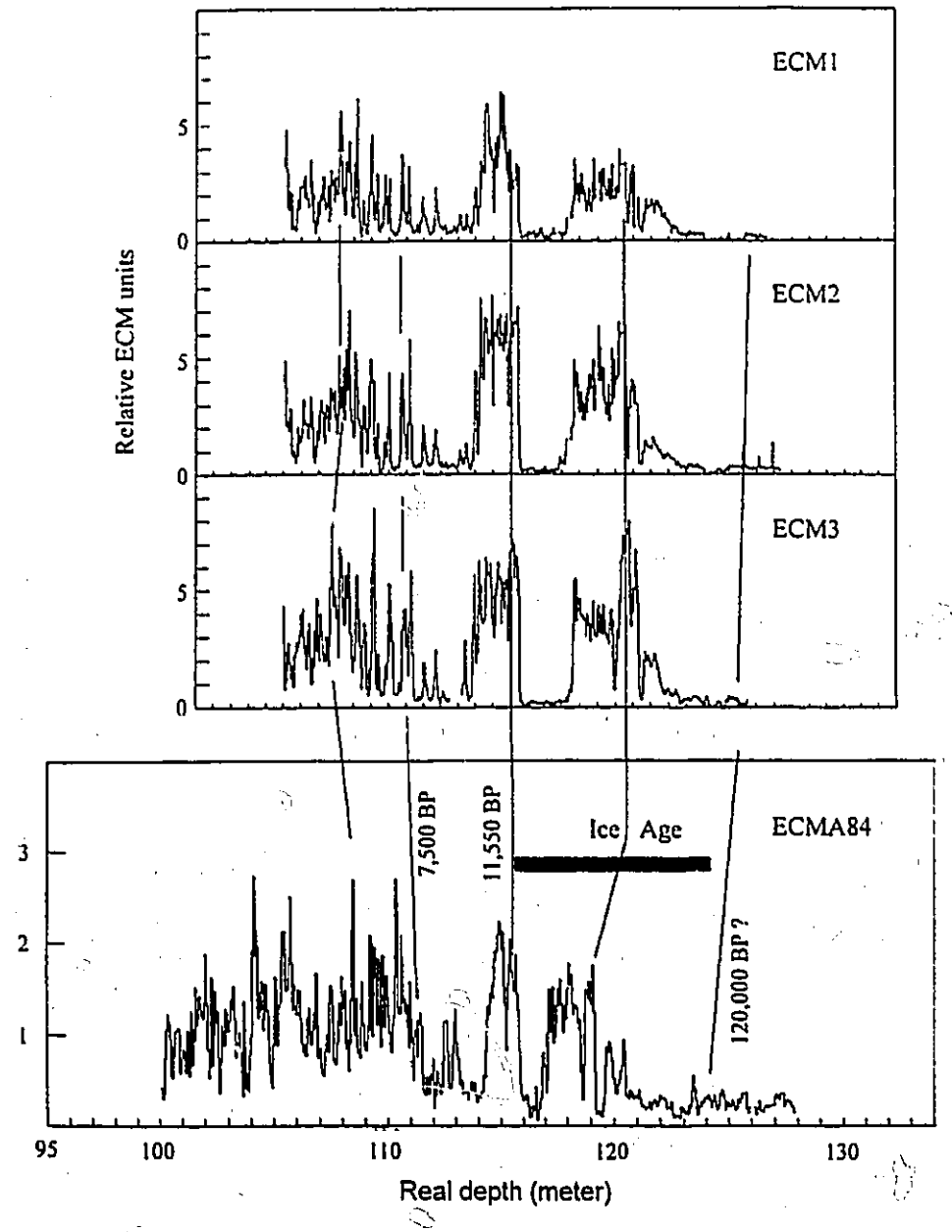

Figure 11a. Bottom ECM details on the A84 and A93 holes. ECM1 stands for A93.1, unprepared; ECM2, A93.1 prepared and ECM3, A93.2, unprepared (After Zheng et al., 1995).

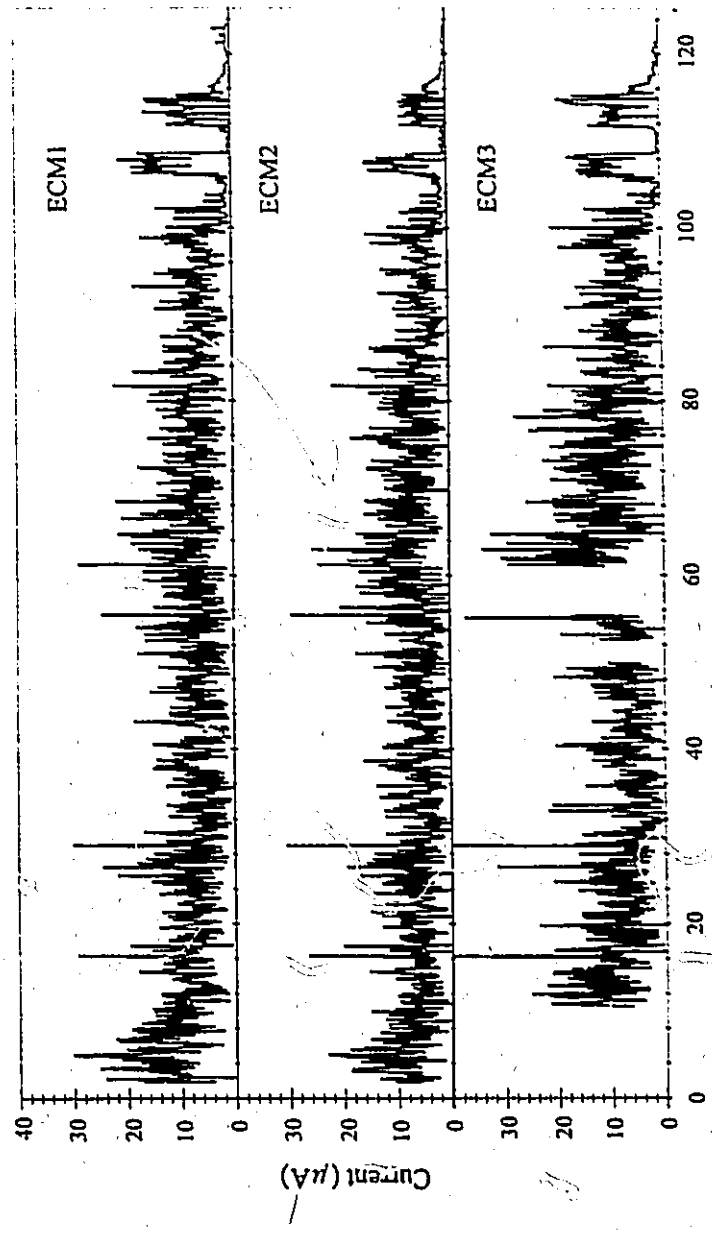

Figure 11b. ECM profiles with real depths, produced by NRC's ECM system. Because the sampling site of the two ice cores is close, the ECM similarity between the two cores can easily and visually be seen.

3.2 Correlation of the A93.1 and A93.2 ECM Records

The full length of the A93.1 core was measured three times, once directly on the unprepared surface and twice on a flat surface made by a band saw subsequently planed by a clean microtome knife. The two data sets on the prepared surface were done using different ECM devices but gave virtually identical results. The data from the prepared surface and the unprepared surface have significant differences and this data is included separately in the analysis. The A93.2 core was measured for ECM only once on the unprepared surface. The three A93 ECM data sets by NRC ECM system (Figure 11b) are referred to as:

A93.1 on unprepared surface ECM1

A93.1 on prepared surface ECM2

A93.2 on unprepared surface ECM3.

Three sections of ECM results (the sore section numbers are #14, #65 and #137) from the IFI system are also included in this thesis. Comparison between the two systems' results will be discussed in Section 3.6.

As a rough check of ECM result qualities, the visual comparison of the ECMs was first cross checked. Figure 11b shows the three ECMs changes with real depths. The ECMs have outstanding similarity. Correlation coefficients between ECM1 and ECM2 and between ECM1 and ECM3 were later calculated. Because the two ice cores were drilled only two metres apart and the depths were virtually the same, 5 cm averaged data were used for correlation analysis. Results show that ECM1 and ECM2 are highly correlated with a correlation coefficient of 0.842 based on 5 cm averaged ECM signals of the whole length series. ECM1 and ECM3 are also well correlated with a correlation coefficient of 0.644 based also on 5 cm averaged ECM signals of the whole length series. However, the variability is obviously larger than that between ECM1 and ECM2. This suggests that ice cores situated as little as two metres apart, could give important differences in electrical conductivity. The details, in this regard, will be discussed in Sections 3.3, 3.4 and 3.5 in this chapter.

The ECM3 record is probably the best because the A93.2 core quality was better than for A93.1 (Refer to Section 2.5). However, two data gaps occur at depth interval/time intervals (52 to 53)/(1439 to 1361 AD) and (58 to 66)/(1243 to 1100 AD) (Figure 9a and b). The ECM2 record was used in some cases to infill these gaps. The ECM time series from these records were then correlated at three different levels of resolution.

The bottom 30 metre of ECM record is given in details for ECM1, ECM2, ECM3 and A84 in Figure 11a. The early Holocene minimum is clearly present in all three records. The beginning and end of Wisconsin glacial period ice is indicated on these ECM plots and shows a very close relationship between the of $\delta^{18}O$ and ECM records in the A84 core record presented in Figure 8a and 11a. Interestingly the strong ECM signal has not been attenuated in all of the Wisconsin ice from A84 (A87 not shown), A93.1 and A93.2, as it is in other Northern Hemisphere cores (Neftel et al.,1985; Hansson, 1994). Ice Age ice (very low $\delta^{18}O$ values and high impurity content) from Greenland, Devon Island and A77 on Agassiz Ice Cap (lower elevation) is alkaline due to carbonate dust, and consequently has neutralized the acids, giving a very low ECM signal. In these cores, the ECM signal shifts abruptly at the end of the Ice Age at the same position as the $\delta^{18}O$ shift. The reasons that this does not happen at the top of the Agassiz flow line has been discussed in Section 3.1.1.

3.3 Correlation of High Resolution ECM Records -- Over the Last 250 years

Using time scale fixed points for volcanic events Katmai, Laki and 1259 AD (at 1912, 1783 and 1259 AD respectively) the ECM1, ECM2, ECM3 1 cm-averaged data were dated, giving a resolution of 10 measurements per year. The 1cm data has sufficient

resolution for only the most recent 250 years of record (to 10 cm annual layer thickness, see bottom bar of Figure 12). The three resulting ECM series are plotted in Figure 13 with the major volcanic events. It is clear that the three series record the major volcanic peaks associated with Laki, Katmai and Tambora, but the smaller events (like Krakatoa) often vary in relative importance. In fact, while Krakatoa can be found in ECM3, it is difficult to identify in ECM2 and can not be found in ECM1. Such differences must be viewed as noise and, if one had only a single ECM series, events like Krakatoa could be lost. This suggests that at least 2 or more ECM records should be used in order to identify smaller events similar to Krakatoa. Moreover, events like Krakatoa can only be separated from noise if a good chronology has already been established.

Ice core derived records, even a few metres apart, are strongly affected by noise of various sorts related to snow drifting, melt and specific variable methodology, as well as on site operation. It is hard to separate the noise sources because usually only one ice core is available from a given site and only one ECM is done. In core A93, ECM2 and ECM1 were obtained less than two centimetres apart on the same ice core. As this is too close for there to be noise from drift or melt, the differences between ECM1 and ECM2 in Figure 13 must be considered as mainly due to micro features such as ice crystallography and the overall methodology.

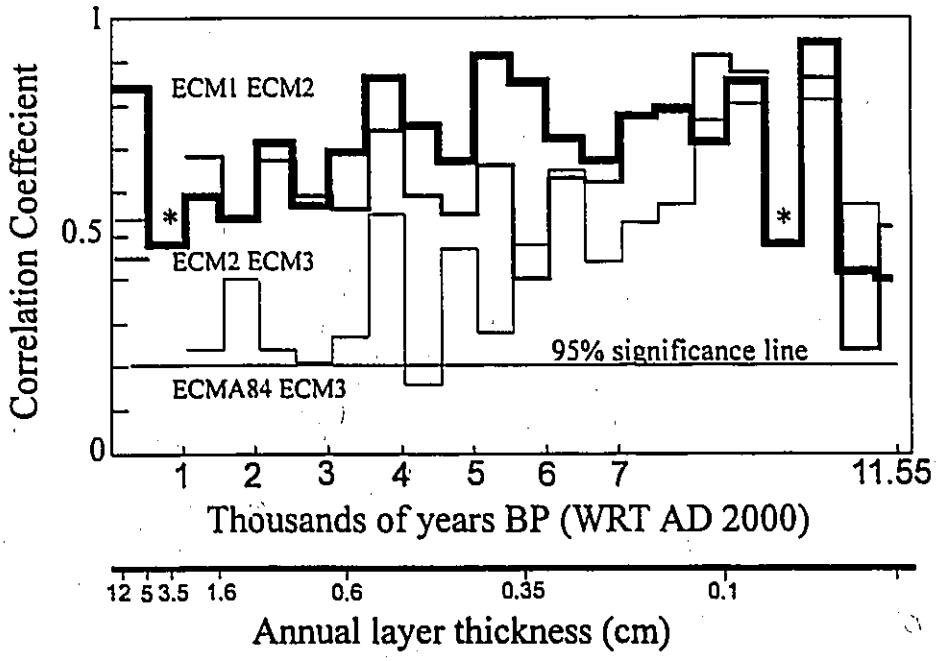

Figure 12. Correlation coefficients of ECM1 with ECM2, ECM2 with ECM3 and ECM3 with ECMA84. Data used in this figure are 5 year-averaged. 500 year segments are used for maximum correlation coefficient by looking 150 years to either side of the nominal segment age for the best fit (After Zheng et al., 1995).

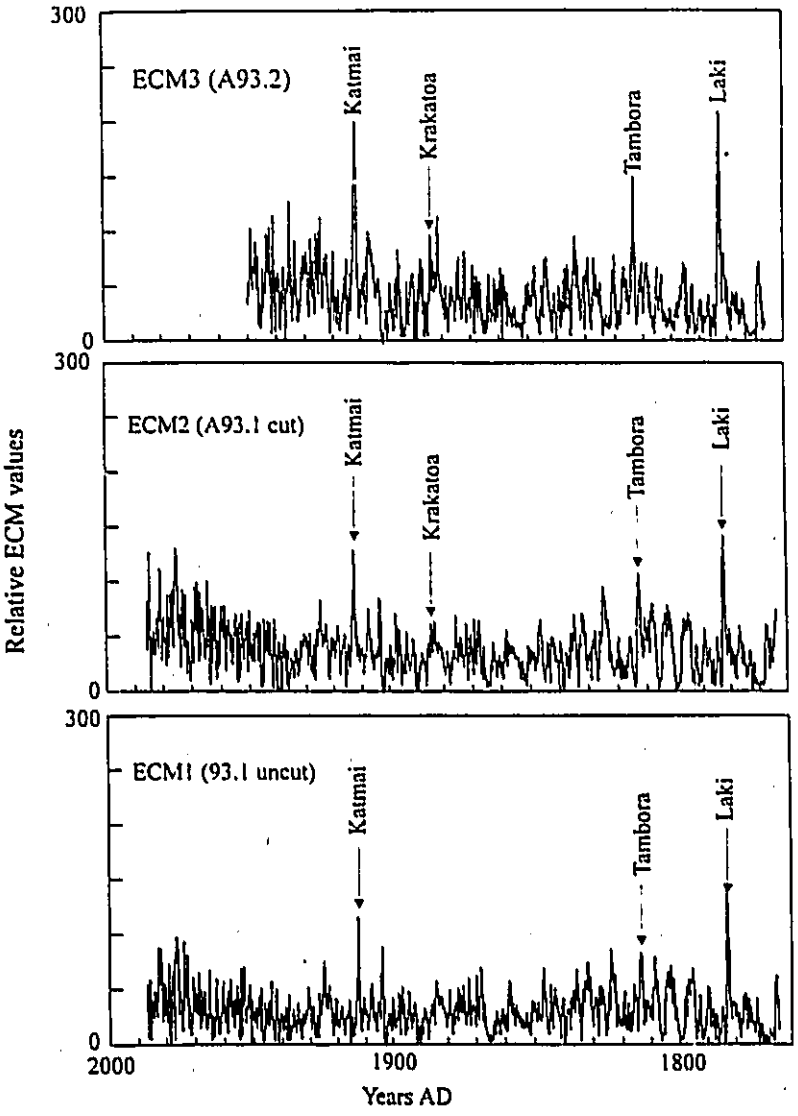

Figure 13. Recent 250 year ECM records on A93 ice cores with 1/10th year samples. Major volcanic events like Katmai at 1912 AD, Krakatoa at 1884 AD, Tambora at 1816 AD and Laki at 1873 AD are marked and compiled in Table 4 (After Zheng et al., 1995).

Figure 14 shows time series of correlation coefficients of ten year segments between ECM1 and ECM2 and between ECM2 and ECM3. These are correlation maxima found by letting the given ten year segment look 5 years to either side of the nominal equivalent time horizon on the other series (ten year segment with +/- 5 lags). There is very little inter-series lag found between these series. If no maximum is found then the coefficient is not used. The two series ECM1 and ECM2 from the same A93.1 core are typically correlated at the 0.7 to 0.9 level meaning that the overall methodological noise accounts for about 10 to 30% of the variability (Fisher et al., 1985). The ECM2 and ECM3 series from two different cores separated by only 2 metres are correlated somewhat lower at the 0.5 to 0.7 level suggesting a total intercore noise level of 30 to 50% of the variability, or a combined drift/melt noise contribution of 20% of the variability for cores this close together. Such stratigraphic noise percents for cores this close together (2m) are similar to the noise percent difference for cores compared at separations of 100's of metres (Agassiz) and up to 100's of kilometres (Greenland) (Fisher et al., 1985; Reeh, 1988). This suggests that stratigraphic noise is important even within a couple of metres.

Violent volcanic ECM signals are outstanding and are usually much larger than the ECM average signals. As can be seen in Figure 8a, the frequency of volcanic events like Laki and Katmai are very low. Those signals can be identified easily and accurately.

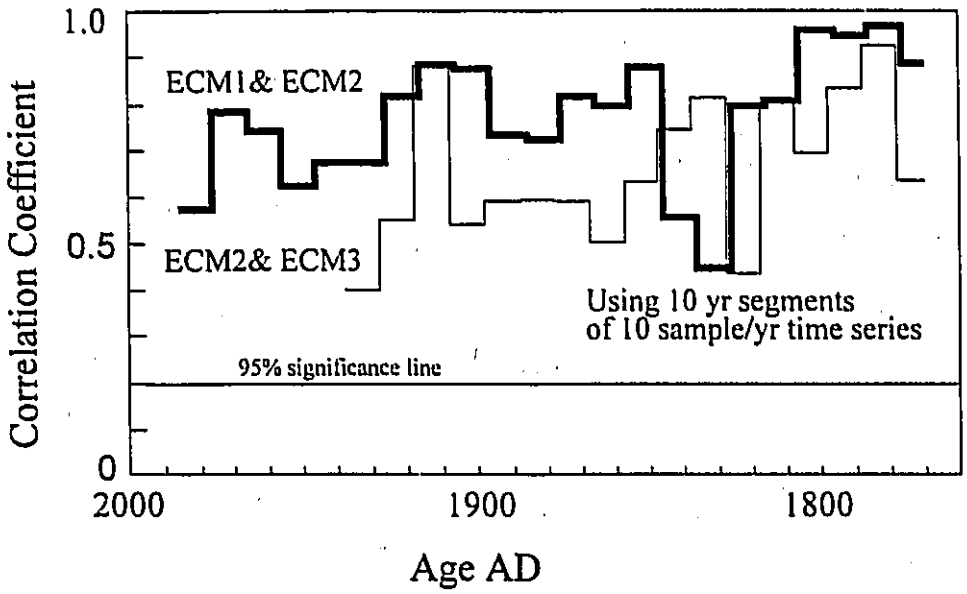

Figure 14. Time series of correlation coefficients of ten year segments between ECM1 and ECM2 and between ECM2 and ECM3 (After Zheng et al., 1995).

In order to confirm the volcanic signals, Frequency Distributions for the recent 240 and 800 years of the three ECM series have been calculated using 10 samples per year data. The results are shown in Figure 15. The shaded plots are for the approximately 240 years and the unshaded curves for the most recent 800 years of 10 samples per year data. The three identified volcanic peaks that are consistent from series to series, Laki, Katmai and Tambora have peak values that have a frequency of less than 0.7, 1.0 and 1.8% respectively in the three ECM series over the most recent 240 years. For Katmai and Laki, the Frequency distribution are smaller than 0.3%. Therefore, the largest peaks could be expected to be correctly identified in most single cores as the three largest peaks in such a time interval, even if the single core was not continuously sampled. Krakatoa on the other hand is an anomaly in only the ECM3 series and would have a large chance of being mis-identified in ECM2 and an even larger chance in the ECM1 series. Such 'intermediate events' can not always be identified from single series that are not continuously sampled and even in cases where there is continuous sampling there is a chance of missing such events.

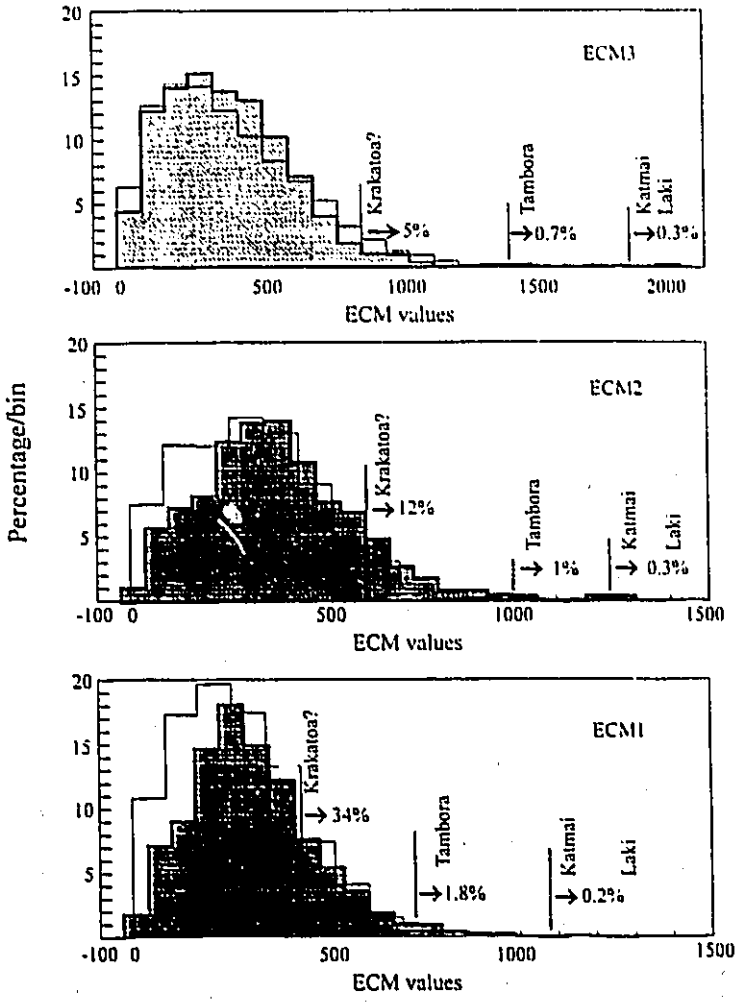

Figure 15. The Frequency probability, expressed as density distribution for the 10 sample per year data. Laki, Katmai and Tambora have very small probabilities, less than 1.8% for Tambora, less than 0.3% for Katmai and Laki in all the ECM records respectively. This suggests that large volcanic events can be easily identified even from a single record. However, for moderate volcanic event like Krakatoa, the signal could be missed (After Zheng et al., 1995).

3.4 Correlation of Lower Resolution--Average Annual Series over the Last 800 Years

A longer Agassiz ECM series can be brought into the analysis using an average annual resolution for the A77 and A84 as well as the A93.1 and A93.2 cores.

The A77 ECM record (Fisher et al., 1995) was done by hand on stored cores two years after they were drilled and after about 1cm of surface ice was scraped away with a clean stainless steel knife. The A77 ECM record is not considered as good a record as the A84 or the A93 records which were done in the field on clean fresh core immediately after they were drilled. Nevertheless the A77 annual average record presented in Figure 16 contains much of the same detail as the other ECM and in particular shows the same major peaks as the others.

The 800 year A77 record is significantly correlated to that of A84 over most of its length, (see plot No. 4 of Figure 17). Figure 16 also shows the A84 and A93.2 (ECM3) annual average series. All these ECM series have had their initial time scales tuned slightly to place the peaks identified with Laki (1783 AD) and the big 1259 AD peak at the correct ages (Hammer et al., 1980; Hammer, 1984; Bourgeois, 1986).

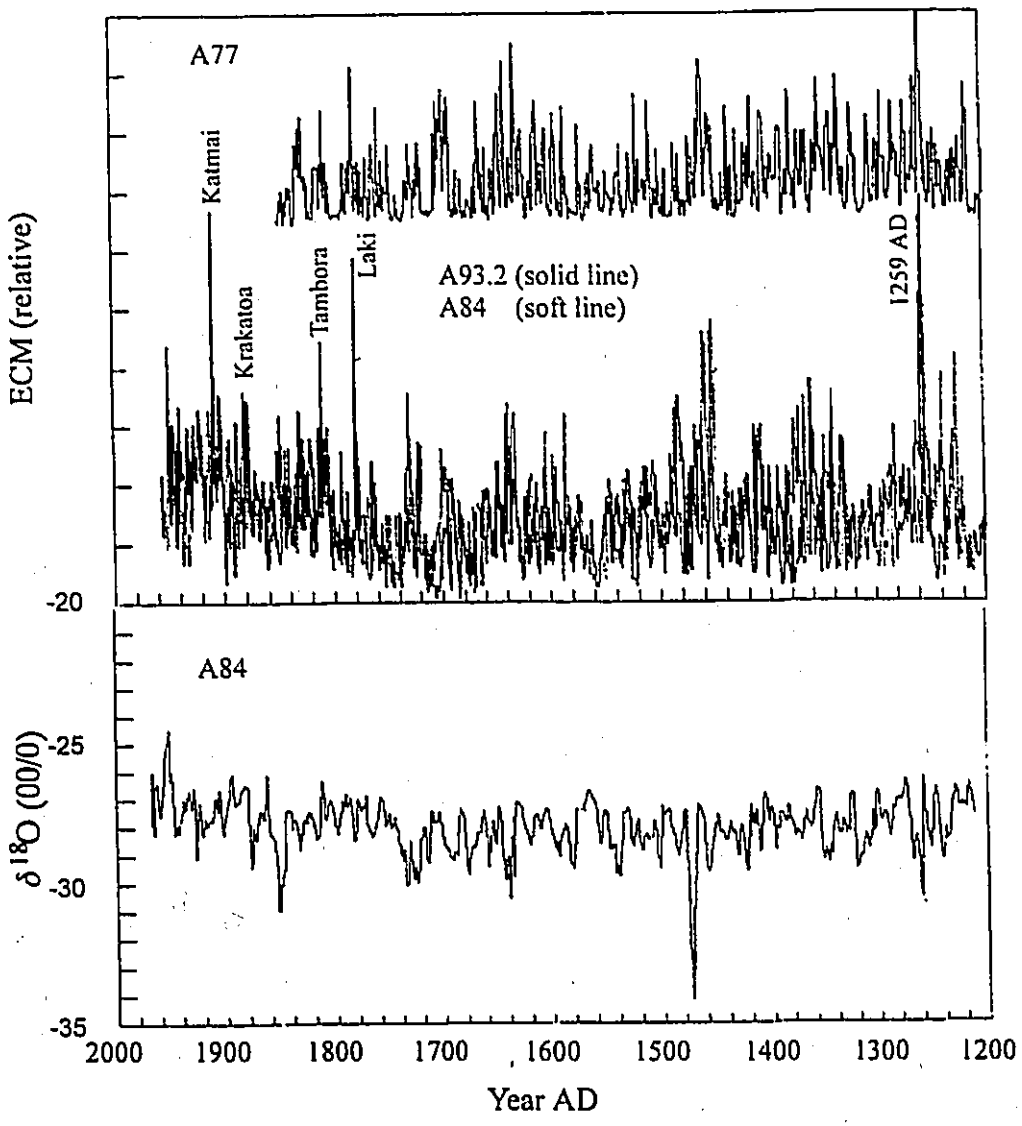

Figure 16. ECM annual average series of cores A84, A77 and A93.2 and the A84$\delta^{18}O$ results (After Zheng et al., 1995).

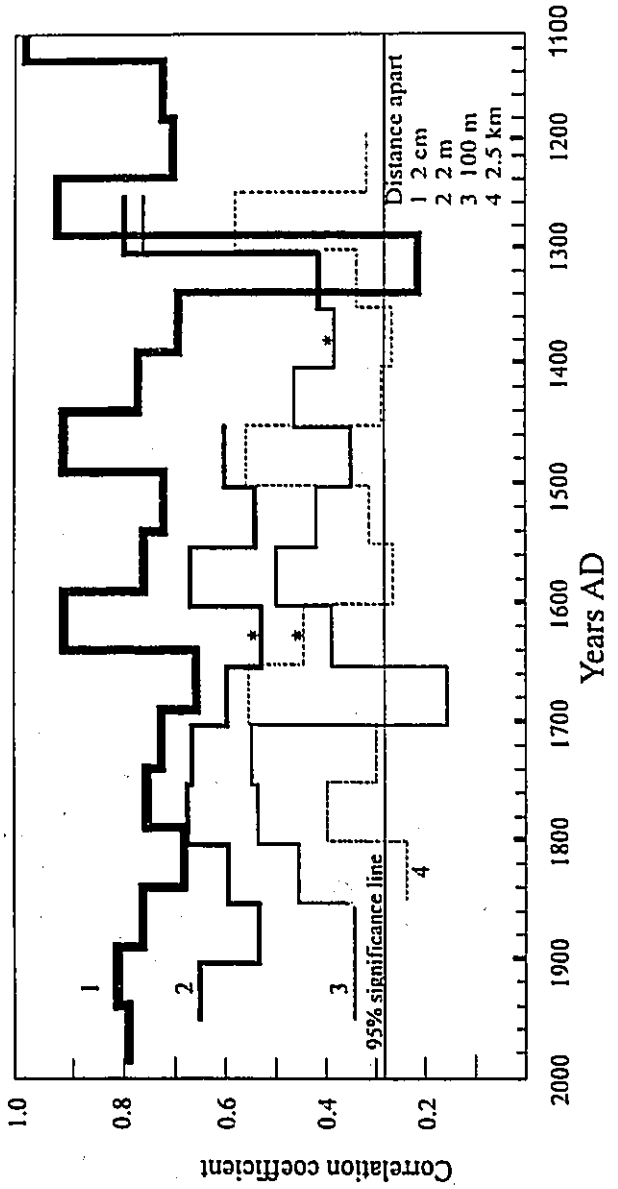

Figure 17. Comparison of correlation coefficient of different ECM annual average records from the Agassiz Ice Cap (For most recent 900 years only)(After Zheng et al., 1995).

A84 and A93.2 (ECM3) are very significantly correlated and virtually all the major and many of the smaller peaks are present in both. Between the fixed time points at 1783 AD and 1259 AD the two series ages can wander relative to each other by up to 5 years. The maximum correlation coefficients for 50 year segments of the series are given in plot #3 of Figure 17. The maximum allowed lag between nominal ages of the two series for the maximum coefficient is +7 years. Only in two cases (marked with a*) could no maximum correlation be found within the 7 years of the nominal ages. One of these cases (AD 1350 to 1400) is where the ECM3 series has a data gap that was infilled from ECM2. It appears in retrospect that the ECM2 data in this range is compromised possibly by a slip in the depth scale in this range during measurement that was not picked up in the computer files(an error of modern data gathering).

The A84 ECM and ECM3 records were normalized (see below) and added together in order to enhance the signal and reduce the noise. This can be done in a number of ways. Here they were added together, 50 year segments at a time, at the points of maximum correlation (a) by holding the A84 time scale as correct, and (b) by assuming the ECM3 time scale is correct. These two 'correlation optimized' series appear in Figure 18a and aside from the relative time wandering between the fixed points these series are virtually identical, except where there was no valid match between 1350 and 1400 AD (the data

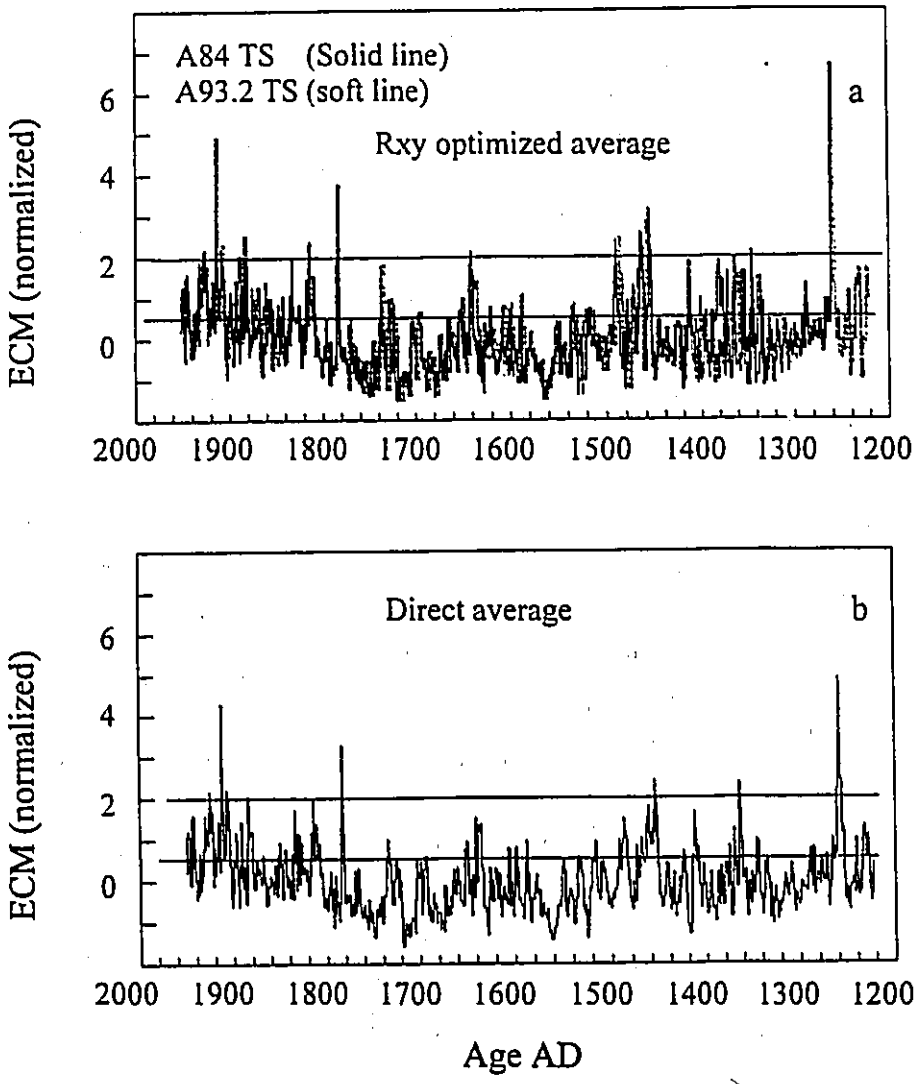

Figure 18. R_{xy} optimized average and direct average of A84 and A93.2 cores (After Zheng et al., 1995).

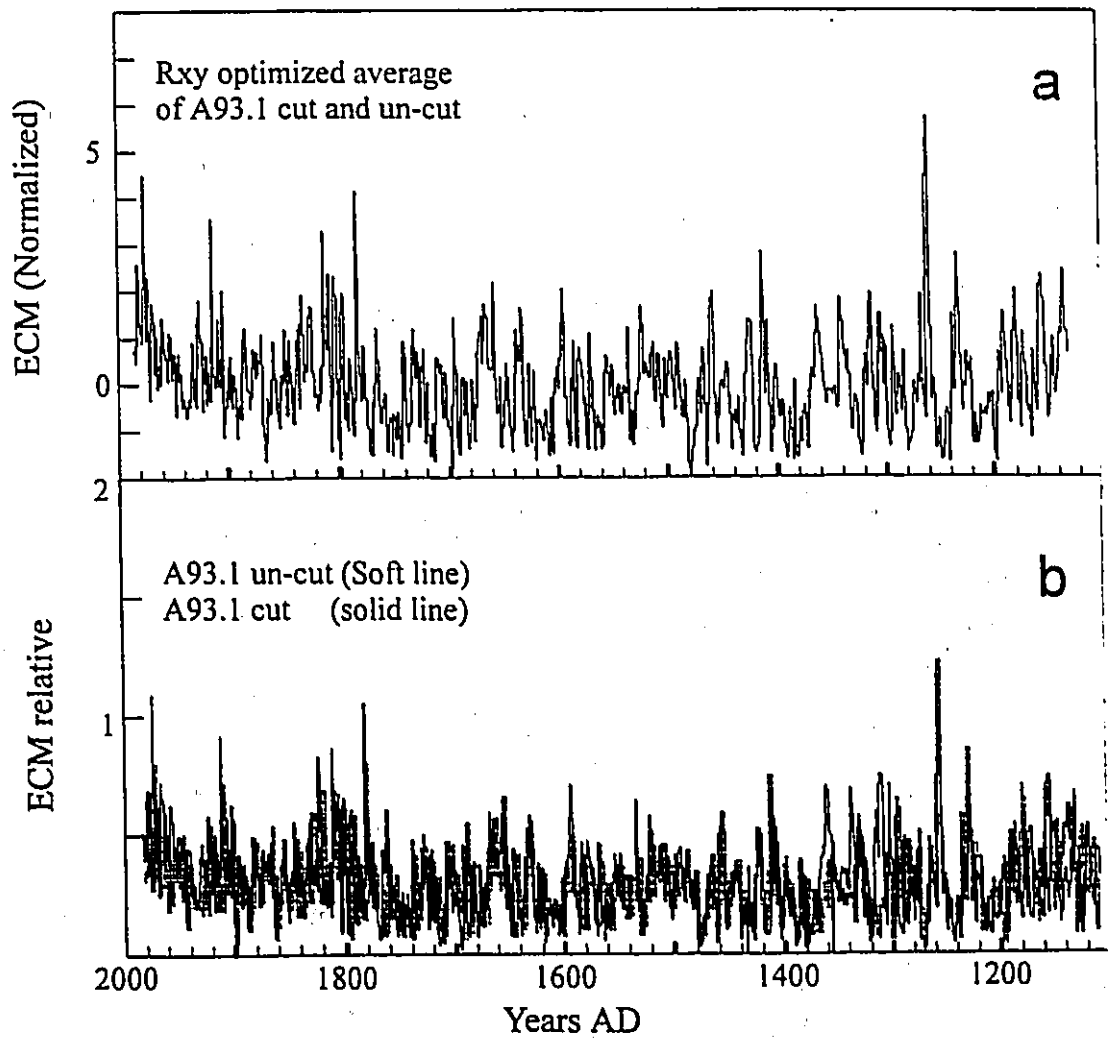

Figure 19. Comparison of recent 900 year ECM results between individual ECM and R_{xy} optimized (50 year segment correlation) averaged ECM series (After Zheng et al., 1995).

gap discussed above). A simple averaging of the series ignores the relative time errors between the fixed points and results in the somewhat attenuated average series of Figure 18b. The segment by segment correlation optimizing method seems best in that it reduces noise, preserves detail and does not exacerbate dating errors between fixed points.

The two A93.1 core records ECM1 and ECM2 appear in Figure 19b and are highly correlated (plot #1 of Figure 17), except from about 1300 to 1380 AD. The problems in this interval seem to be with the ECM2 data, as already mentioned above. The 50 year segment correlation optimized series is presented in Figure 19a.

The ECM3 versus ECM2 maximum correlation coefficients appear as plot #2 in Figure 17. Inspection of Figure 17 shows the obvious expected result that the correlations and intercore signal percent falls off with distance apart. The 95% significance line is drawn in and almost all of the 50 year segment correlations between any pair of series fall above it. Plot #4 correlating A77 with A84 could be too low because of the lower quality of the A77 data.

Finally Figure 20 shows two simple "grand averages" of the normalized series. One includes the A77 data and one excludes it. There is the inevitable smearing due to

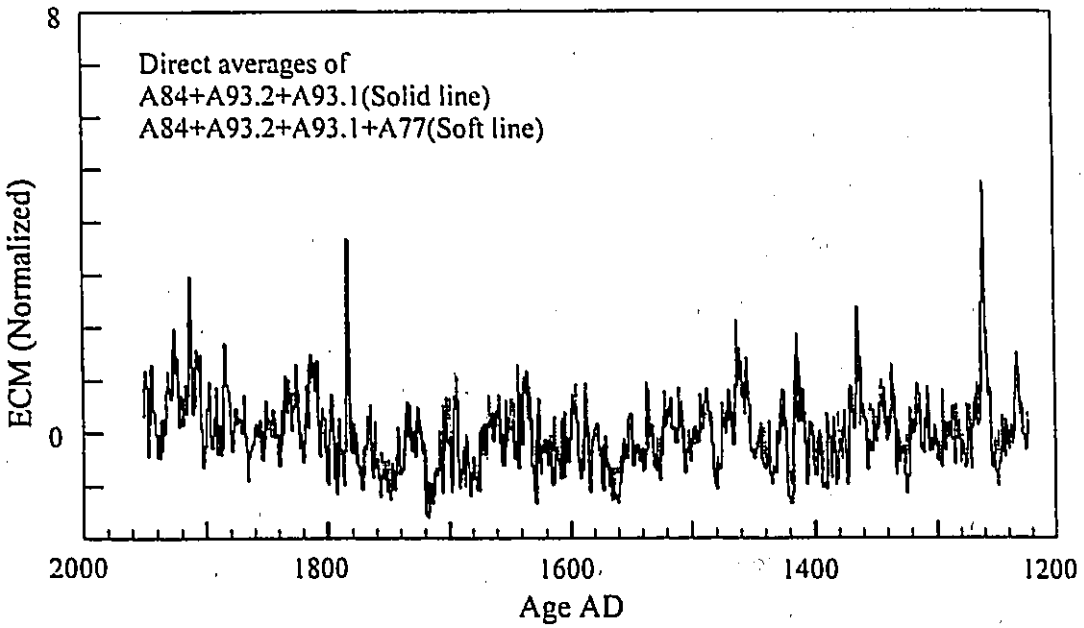

Figure 20. Comparison of two simple "grand average" of the normalized series with and without A77 ECM series (After Zheng et al., 1995).

relative inter-core age errors but one would expect that the "grand average" major highs and lows to be much reduced in noise.

3.5 Lower Resolution -- Five Year Average of Holocene ECM Records

The Holocene ECM records for the A93 cores have been assigned ages from an initial theoretical time scale then tuning the A93 ECM time series to those of previously dated cores A77, A84 and A79 ECM series (Fisher et al., 1983; Fisher et al., 1995). Table 4 gives the A84 time scale fixed points.

There is a period in the early Holocene when the melt percents in A84+A87 are very high (>40%, Koerner and Fisher, 1990). Such high melt percents have been interpreted to represent average summer temperatures 2 °C higher than present (Koerner and Fisher, 1990). This clearly had a profound effect on the acidity or ECM, which had very low (alkaline) values during the early Holocene. The early Holocene melt layer percents are consistently high enough to suspect that the overall mass balance and thickness of the ice cap was significantly reduced from present, making the time scale for the early Holocene difficult to estimate (Fisher et al., 1995).

Three correlation plots appear in Figure 12, (ECM1 vs ECM2, ECM2 vs ECM3 and ECM3 vs ECM A84) again using the optimized or maximum correlation coefficient. In this case, 500 year segments of the 5 year average series were used, looking 150 years to either side of the nominal segment age for the best fit. Where there are data gaps there are gaps in the correlation series. There is also a correlation gap in ECM3 where melt has attenuated the signal and no matches were possible. Except for these cases all the correlations are significant at the 95% level (horizontal line), when allowance is made for reductions in degrees of freedom due to the first autocorrelation (WCD, 1992). Some of the major volcanic events like 1259 AD, and Eldgja AD 934 come through as 'visible' in the 5 year average series of Figure 9 but some other major eruptions like Laki do not. This and the significant differences between ECM1, ECM2 and ECM3 are probably due in part to the annual layer thickness decreasing under that needed to define an accurate 5 year average in the early Holocene. The annual layer thicknesses consistent with the time scale appear in the bar at the bottom of Figure 12.

3.6 Comparison of two ECM systems

Both ECM systems from NRC and IFI were used for the 93.1 ice core on cut surface. The two systems were manufactured separately without any collaboration before the field

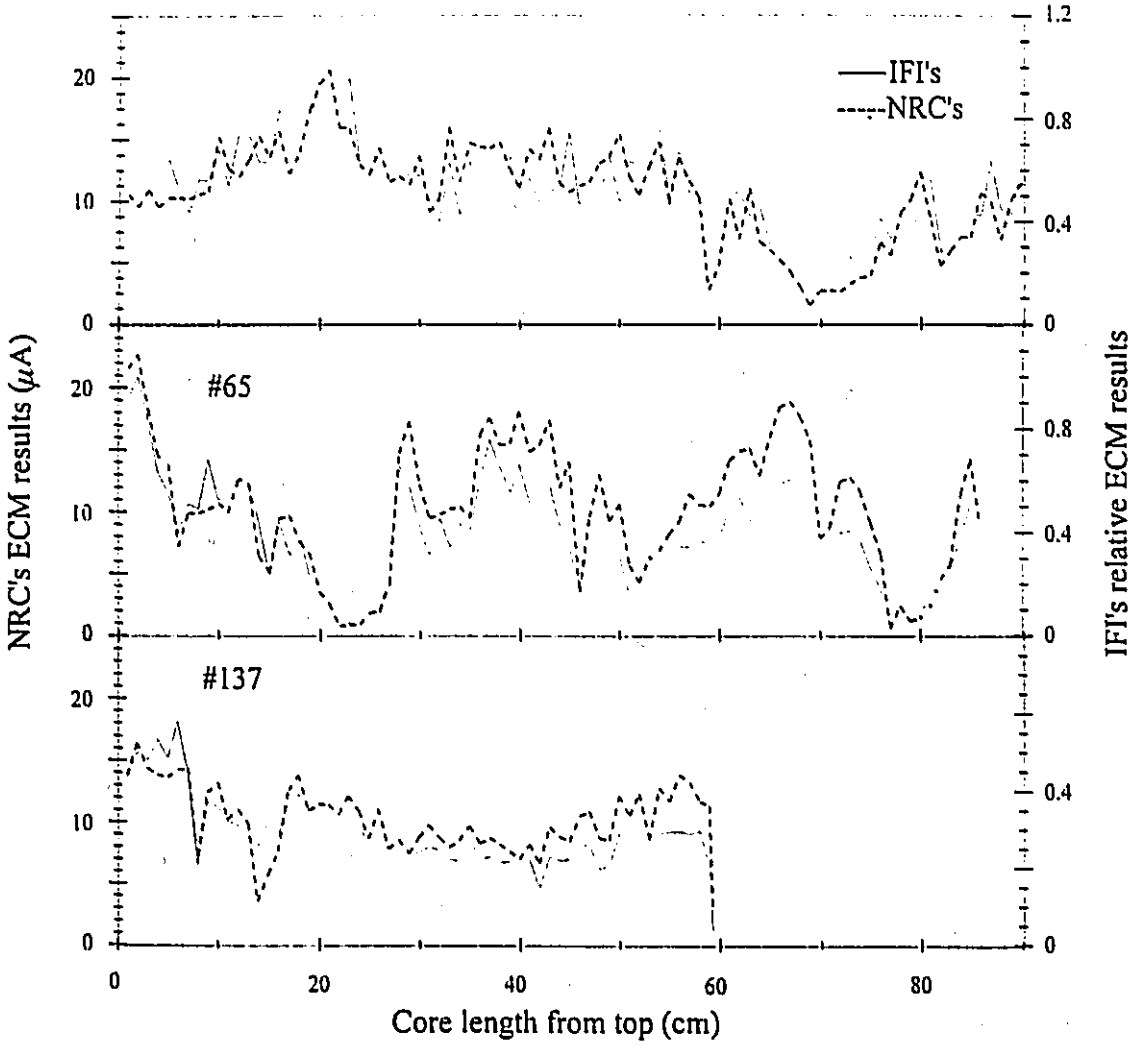

Figure 21. ECM result comparison between the two ECM systems from IFI and NRC. Correlations between the result sets gives coefficients of 0.80, 0.91 and 0.79 for ice core sections #14, #65 and #137 respectively.

work. About 10 section ECM results were visually compared on site during the field trip. This inspection showed no apparent difference in the two measurement systems. More detailed examination on sections #14, #65 and #137 of the Core 93.1 were done on the cold laboratory after the field work. Sections #14 and #65 are continuous one piece sections while #137 is a 7 piece section. Results from the two systems have essentially no remarkable difference. One centimetre averaged data have been plotted in Figure 21. The cross correlation calculation gave coefficients of 0.80, 0.91 and 0.79 respectively for the three sections of the ice core. The 10 to 21% variability should come from the crystallography and methodology as discussed in the ECM comparison on prepared and unprepared surfaces. The correlation coefficients of ECMs between two ECM systems and between prepared and unprepared surfaces are the same. This suggests that the variability may only come from the crystallography of the ice core and electronic noise, and not from the ECM system itself. Thus, ECM results from different ECM systems can be compared if the ECM systems are similarly designed.

3.7 Summary of the discussion

Our data show that ECM signals from prepared and unprepared surfaces of the same ice cores are very similar even though detailed ECM signal differences exist. The correlation

coefficient between the two ECM series of whole length A93.1 ice core from prepared and unprepared surfaces is 0.842, which suggests that ECM could be carried out directly on the newly mechanically recovered ice core without creating a new surface, if care is taken during the core handling and ECM processing. Correlation analysis of high resolution ECM records from the A93.1 prepared and unprepared surfaces over the last 250 years shows that 10 to 30% of the variability is unexplained by the linear correlation, but could be attributed to methodological noise and ice crystallography.

Ice cores taken only two metres apart have a very similar ECM trend and major ECM peak locations. The correlation analysis gives a coefficient of 0.644 between the two whole length ice cores. Correlation analysis of high resolution ECM records from the A93.1 prepared and A93.2 unprepared surfaces over the last 250 years gives a 30 to 50% variability. This suggests that there is an additional source of variability, perhaps a combined drift/melt noise.

ECM results from two ECM systems are highly correlated with a coefficient of larger than 0.79. The existing variability between results from the two ECM systems is similar to that between the ECM results on the prepared and unprepared surfaces of A93.1 core. That, in another way, suggests that the methodology and the crystallography count for

about 20% variability.

4. Review of Palaeoclimatic records from Canadian Arctic

Ice caps in the Canadian High Arctic, such as those ice caps on Devon, Ellesmere and Axel Heiberg Islands are much thinner than the glaciers on Greenland and Antarctica. However, Arctic ice caps can provide climatic records comparable in length with those obtained in Greenland and Antarctica though such records are much less detailed because over 90% of the time period is confined to the bottom few metres of ice. Studies on ice cores from the Canadian High Arctic revealed that the age of large ice caps is about 100 ka to ~130 ka (Paterson et al., 1977; Fisher and Koerner, 1986; Koerner, 1989), and contain ice from the last glaciation in their lower layers plus interglacial ice beneath that. Thus although these ice caps are dominated by Holocene ice, they represent a wide time period from the last interglacial to present, which covers a little more than the oxygen isotope stages from 1 to 5 in the marine oxygen isotope stratigraphy (Dawson, 1992). Because it is feasible to drill more than one hole in shallow ice caps to check the common assumption that a single core provides a climatic record representative of a wide area, relatively large numbers of ice cores have been recovered from the Canadian High Arctic ice caps such as Devon, Agassiz and Meighen since the 1960's (Fisher, 1983; Koerner, 1989). Analysis of several profiles of ice cores can provide more accurate and precise information about the palaeoclimate during the Holocene and pre-Holocene.

4.1 Holocene $\delta^{18}O$ records

Figure 22 shows the Holocene ice core $\delta^{18}O$ records from Ellesmere Island, Devon Island and Greenland (Fisher and Koerner, 1979, 1994; Fisher et al., 1983; Koerner et al., 1987; Fisher, 1987; Koerner, 1989; Fisher et al., 1995). Data used here are all 25 year averages with the exception of Devon D72+73 data which are 50 year averages. Some common features, such as the steady decrease of $\delta^{18}O$ in the last 9000 years; the relatively sharp increase in the recent 100 years and the $\delta^{18}O$ deep drop resulted from the Little Ice Age, can easily be seen for the four Agassiz ice core records from the figure while the results from Devon Island and Greenland show different pictures. Those features will be discussed one after another together with the results from Devon Ice Cap and Greenland; and ECM and/or summer melt percentage data from Agassiz Ice Cap.

4.2 Records between 100 and 9000 year BP

All records from the Agassiz Ice Cap show a decrease in $\delta^{18}O$ starting about 9000 years ago. This decrease suggests that the cooling started at about that time. The results of $\delta^{18}O$ linear regression in that time period, covering 8900 years between 100 and 9000 year BP, are shown in Table 5. The decreasing slopes of the regressions varied from 0.024 to

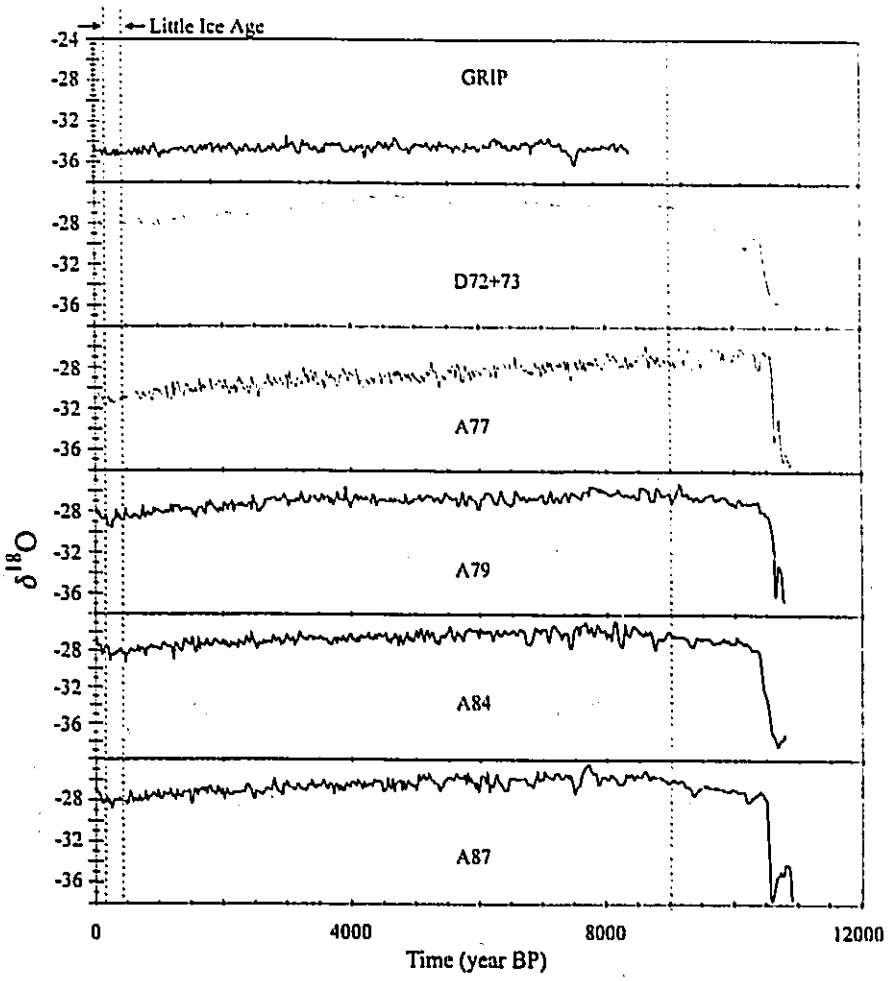

Figure 22. Holocene $\delta^{18}O$ records for A77, A79, A84 and A87 from Agassiz Ice Cap and D72+73 from Devon Ice Cap. $\delta^{18}O$ decreases for 4 Agassiz cores ranges between 0.024 and 0.042‰ per 100 year with an average of 0.029‰ per year. A temperature change of 4.19°C can be translated from the $\delta^{18}O$ change during the last 9,000 years. Several common features for the Agassiz records can be recognized. See text for more details (Modified from Fisher et al., 1995).

Table 5. Linear regression results for the 4 Agassiz ice cores.

Distance From dome		Present to 900 years BP a	b	9000 to 15000 years BP C	D	Temp. change
2.55	A77	-30.7951	0.00042	-32.0683	-0.000538	6.029
1.35	A79	-28.0772	0.000241	-20.1111	-0.000066	3.460
0.2	A87	-27.7071	0.000264	-17.0161	-0.00099	3.790
0	A84	-27.7496	0.000242	-21.3826	-0.00056	3.474
Average		-28.5823	0.000292	-22.6445	-0.000539	4.188

Regression Equation: $\delta^{18}O = -28.5823 + 0.000292 \times time$

At 100BP: $\delta^{18}O = -28.8831$

At 9000BP: $\delta^{18}O = -25.9543$

$\Delta T = \Delta\delta^{18}O/0.62 = (-25.9543-28.5531)/0.62 = 4.192\ ^{o}C$

0.042 ‰ per 100 year with a four-record average of 0.0292 ‰ per 100 year. Using the classic relationship between $\delta^{18}O$ and temperature, $\delta^{18}O = bT + a$ where b is a constant of 0.62 ‰ and a is a constant determined for a region (Dansgaard et al., 1973) and data in Table 5, one can calculate a temperature change of 4.19°C between 100 year BP and 9000 year BP. $\delta^{18}O$ decrease in the last 9,000 years reflects the climate deterioration, which coincides with the Ritchie's pollen record from west Canadian Arctic (Ritchie et

al., 1983).

Figure 22 also shows that four $\delta^{18}O$ records are not exactly the same even though they have the same trend and pattern. Records varied with sites. A77 site, which is supposed to have the "warmest" $\delta^{18}O$ results due to its lower altitude, has the "coldest" $\delta^{18}O$ records. A84 and A87, which are very similar to each other, are supposed to be the coldest in the group but actually have the "warmest" $\delta^{18}O$ records in the group. The reason for this is mainly wind scouring. Fisher et al. (1983) found that the accumulation on the A79 side of the crest is only ~ 65% of that at A77. They believed that most of the scouring occurred in winter because there were more katabatic winds, and because snow gains were smaller and took much longer to compact in winter than in summer. Therefore, more snow on the crest area was blown away in winter and the higher location (^{18}O-depleted) snow was deposited in the lower A77 site, thus biasing the $\delta^{18}O$ records. Further studies (Fisher et al., 1995) on the difference in those $\delta^{18}O$ records using modern accumulations and a flow model explained the ice origin at the different ages along the ice cores.

4.3 Records from present to 400 BP

The Little Ice Age cold period as recorded in the ice cores (See Figure 22) occurred from about 140 to 420 years BP (AD 1570-1850) (Koerner, 1989). The coldest part occurred about 340 years BP (AD 1650). This cold period resulted in a drop in $\delta^{18}O$ starting at about 400 years BP until 100 years BP. All the $\delta^{18}O$ ice core records including those from the Devon Ice Cap from the Canadian Arctic show this event. However, GRIP $\delta^{18}O$ records do not show any significant $\delta^{18}O$ drop during this time period (Figure 22). It can not be decided, up to now, whether this is because the Little Ice Age is localized or whether some unknown factors biased the results. However, the difference between the $\delta^{18}O$ values in sites A77 and A79 is reduced during the Little Ice Age, which might indicate a reduction in scouring (Fisher et al, 1983).

In the recent 100 years, the climate has been significantly warming up. All Arctic records show a sharp $\delta^{18}O$ increase of about 1 to 2 ‰. This increase may come from two fold reasons. One is that CO_2 has been dramatically increasing from about 280 ppmv before the industrial revolution to about 350 ppmv (Keeling et al, 1989) due to human activities, which may have increased the global temperature about 1°C (Bamola et al., 1978, 1983, 1987; Wahlen et al., 1991). The other is that the natural climate warming over this period could occur. However, this has not yet been quantified.

All Agassiz ECM amplitudes in the same time period are also high. They mainly resulted from pollutants like sulphuric acid and nitric acid, which are the major conductors to the ECM signal. Clausen and Langway (1989) concluded that today's yearly deposits of sulphuric and nitric acid are 4 and 2 times respectively, the yearly amount deposited prior to A.D. 1900 and A.D. 1950 respectively after they measured those components in carefully dated ice cores from the Dye 3 region in S. E. Greenland. Here, a $\delta^{18}O$ increase does not directly come from the pollutants themselves but comes from the pollution effect on climate, while the ECM increase does directly come from pollutant concentration increase (mainly from acid concentration).

4.4 Climate in the early Holocene

The Younger Dryas cooling lasted for more than 1,000 years from about 10,000 to about 11,000 years BP (Grant, 1989; Crowley and North, 1991; Dawson, 1992; Alley et al., 1993). This age is mainly based on ^{14}C dating on different materials. The timing for this event could vary a little bit for different locations in the world. The timing for end of the Younger Dryas was thought to be about 10,000 to 10,700 years BP (Paterson et al., 1977; Koerner and Fisher, 1979) but recent dating on this event gives it an age from 11,000 to 11640 years BP (Johnsen et al., 1992; Alley et al., 1993), most likely at 11,500+/-200

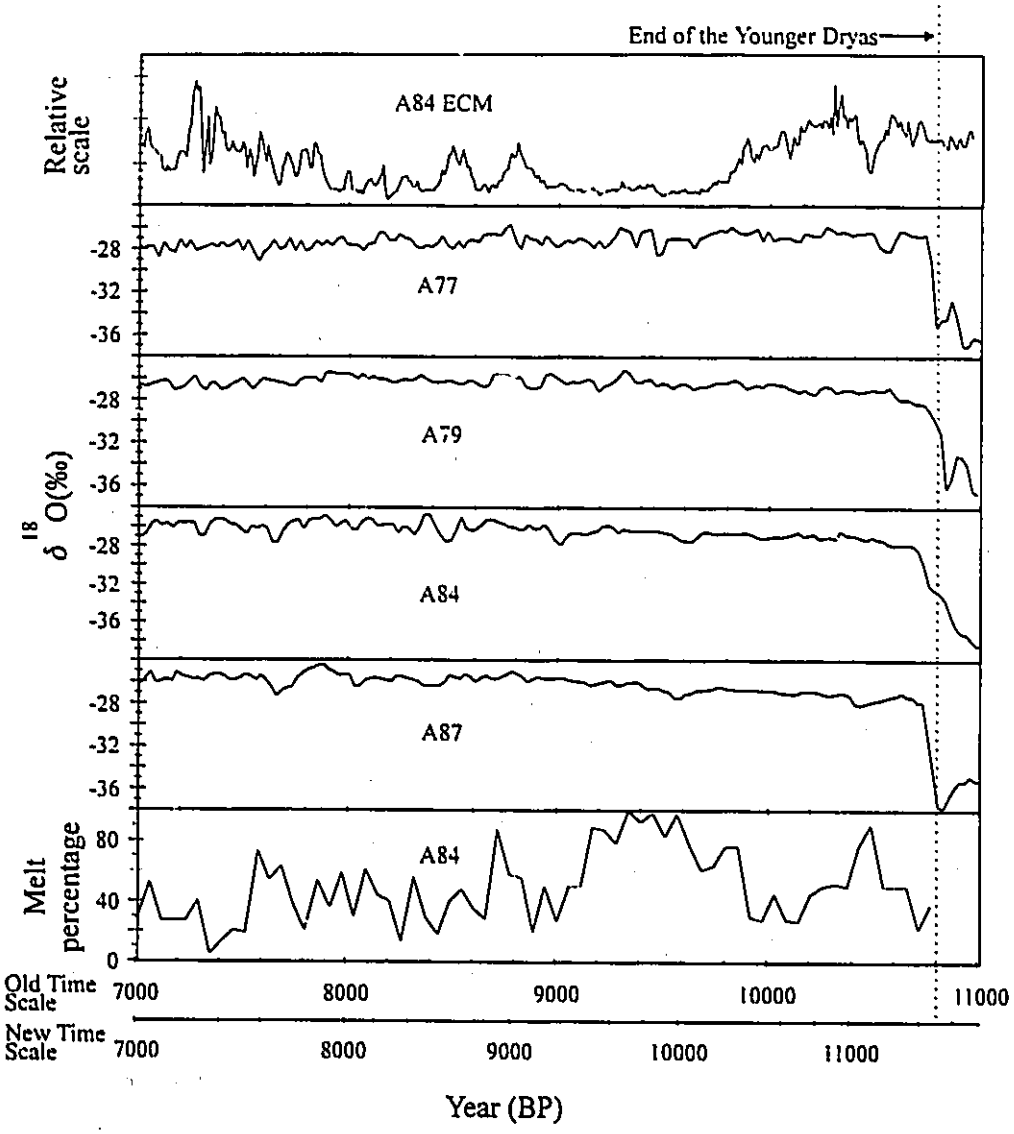

Figure 23. Climate records in the earlier Holocene from the Canadian High Arctic. Accompanied are A84 10 year averaged ECM results and A84 50 year averaged melt percentage (Modified from Fisher et al., 1995).

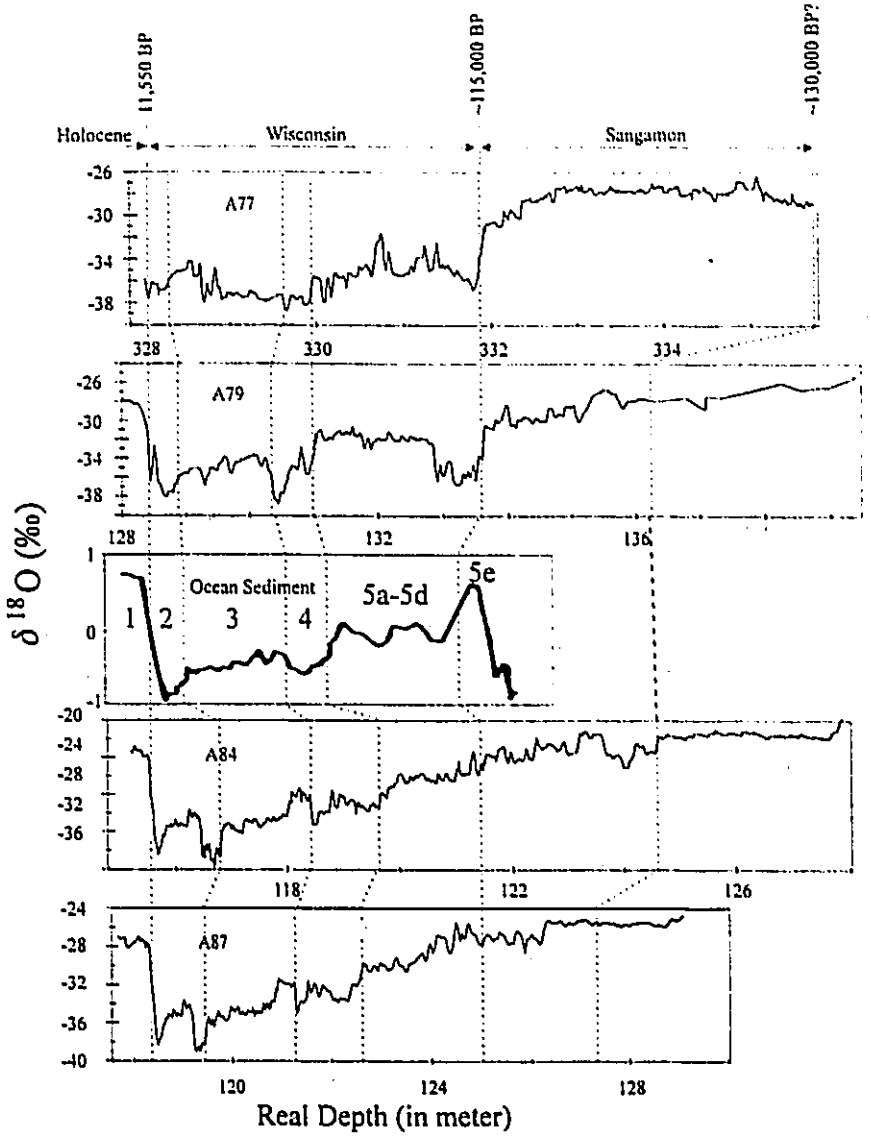

Figure 24. Pre-Holocene $\delta^{18}O$ records from Agassiz Ice Cap of Canada. The records can be divided into 1 to 5 $\delta^{18}O$ stages similar to the ocean sediment $\delta^{18}O$ records (Ocean sediment record is modified from Martinson et al., 1987 and A79 records, modified from Koerner et al., 1987; other data are from Fisher et al., 1995).

years BP based on the GRIP and GISP2 ice core results (Alley, 1993).

All ice core $\delta^{18}O$ records in Figures 23 and 24 show a clear deep drop at the Younger Dryas cold period (Fisher et al., 1983; Fisher, 1987). However, $\delta^{18}O$ records between 9,000 BP and Holocene-Ice Age transition (11,550 BP) have a different $\delta^{18}O$ pattern from that in the recent 9,000 years. Three (those from A79, A84 and A87) out of four $\delta^{18}O$ records on the Agassiz Ice Cap show an increasing trend between 9,000 and 11,550 BP while A77's shows an almost constant $\delta^{18}O$ record. No available data can fully explain the situation yet. However, Fisher et al. (1995) suggested the ice between about 8,000 and 11,550 BP was far from its modern steady state after they carefully studied the $\delta^{18}O$ records of A77, A79 and A84. From the transition to about 9,000 BP, the thickness was reduced. The maximum melt percentage and the ECM minimum occurred at about 10,000 years BP, on one hand, are well preserved in the ice cores (Referring to Figure 24), which suggests that the area was not in the ablation zone, at least not for a long time in the ablation zone. However, on the other hand, the 100% melt percentage, high $\delta^{18}O$ noise and the discontinuities of $\delta^{18}O$ in the 8,000 year BP (Fisher et al., 1995) to the transition interval suggests that part of the records in that time period were ablated (Koerner and Fisher, 1990). Therefore, the thickness was reduced from the transition to about 8,000 year BP, some of the very early Holocene ice might even be missing (Fisher

et al., 1995).

Note from the Figures 8a, 8b, 9 and 25 that the ECM records for A84, A87, A93.1 and A93.2 do not show a drop at the $\delta^{18}O$ transition as in the results from the European Greenland Ice Core Program (GRIP), and the U.S.-Greenland Ice Sheet Project (GISP2) (Taylor et al., 1993), A77 and A79 (Fisher, 1987) records. Possible reasons for this are discussed by Fisher (1987). Fisher found that the enhanced flow of late Wisconsin ice as inferred from hole closure data is negatively correlated with ECM attenuation. He suggested that over time, recrystallization concentrates the acid impurities into a quasi-liquid layer at grain boundaries and at the same time, increasing total strain develops a c-axis alignment. The recrystallization process should be downward based on the temperature gradient at this depth. Therefore, the impurities would be gradually moved downward some distance (about 20 cm), which results in the ECM drop at about 20 cm lower than the transition zone.

4.5 Pre-Holocene records

Pre-Holocene $\delta^{18}O$ records for A77, A79, A84 and A87 are plotted in Figure 24. The A79 record is modified from Koerner (1989) and A77, A84 and A87 data are from Fisher

et al. (1995). Accompanying ocean sediment $\delta^{18}O$ records (SPECMAD) are modified from Martinson et al. (1987). As shown in Figure 24, similar stages to the ocean sediment $\delta^{18}O$ records can be identified. The age at Wisconsin-Holocene transition, that is the transition between Stages 1 and 2, is dated to be 11,550 year BP by correlation with Greenland records (Johnsen et al., 1992). This transition is very sharp in all the records. The transition time could be several decades or less (Dansgaard et al., 1989; Johnsen et al., 1992; Alley et al., 1993). The transition after 5d has an age of 115,000 year BP, by referring to the new Camp Century record (Koerner et al., 1989). The ice age, from 115,000 to 11,550 year BP, has continuously "cold" oxygen isotope values throughout, which suggests the ice age was colder than its nearby climatic episodes, Holocene and Sangamon. Isotope Stage 5e is the Sangamon interglacial, which has Holocene-like or higher $\delta^{18}O$ values.

Stage 2 ice is characterized by very negative oxygen isotope values, relatively high micro particle and calcium concentrations, and "soft" (different rheological properties from the ice above and below) (Fisher and Koerner, 1986; Koerner, 1989). The high micro particle and calcium concentrations suggest that there was high atmospheric turbidity at that time. The presence of calcium suggests that continental shelves were exposed during the periods of low sea level. About a 120 metre lower than present sea level can be estimated

(Shachleton, 1987) during that time period, mainly due to extended periods of cold climate which resulted in a larger amount of ocean water being transferred to the glaciers. Borehole closure rates and tilt were measured high at these age layers on the Devon and Agassiz Ice Caps, which was caused by the relatively high particle concentrations.

Referring to Figure 25, ECM during the ice age period did not fully reach a minimum during the whole glaciation period. ECM only at the Glacial maximum (Stage 2) was reduced to a minimum. Normally, continental shelf material is calcium carbonate rich and calcium is alkaline which causes a ECM reduction. The general steady decrease of $\delta^{18}O$ with abrupt ECM shifts may suggest that the temperature was gradually decreasing (even though some 'big' variations exist, the trend is always decreasing) while the atmospheric circulation system had some sudden realterations during the last glaciation in the Canadian High Arctic, which could totally change the continental shelf calcium carbonate flux in the area.

Bottom parts of the Agassiz cores are "dirty", silt-laden ice (Fisher and Koerner, 1986; Koerner et al., 1987; Fisher, 1987; Koerner, 1989). Radio-echo sounding indicates that

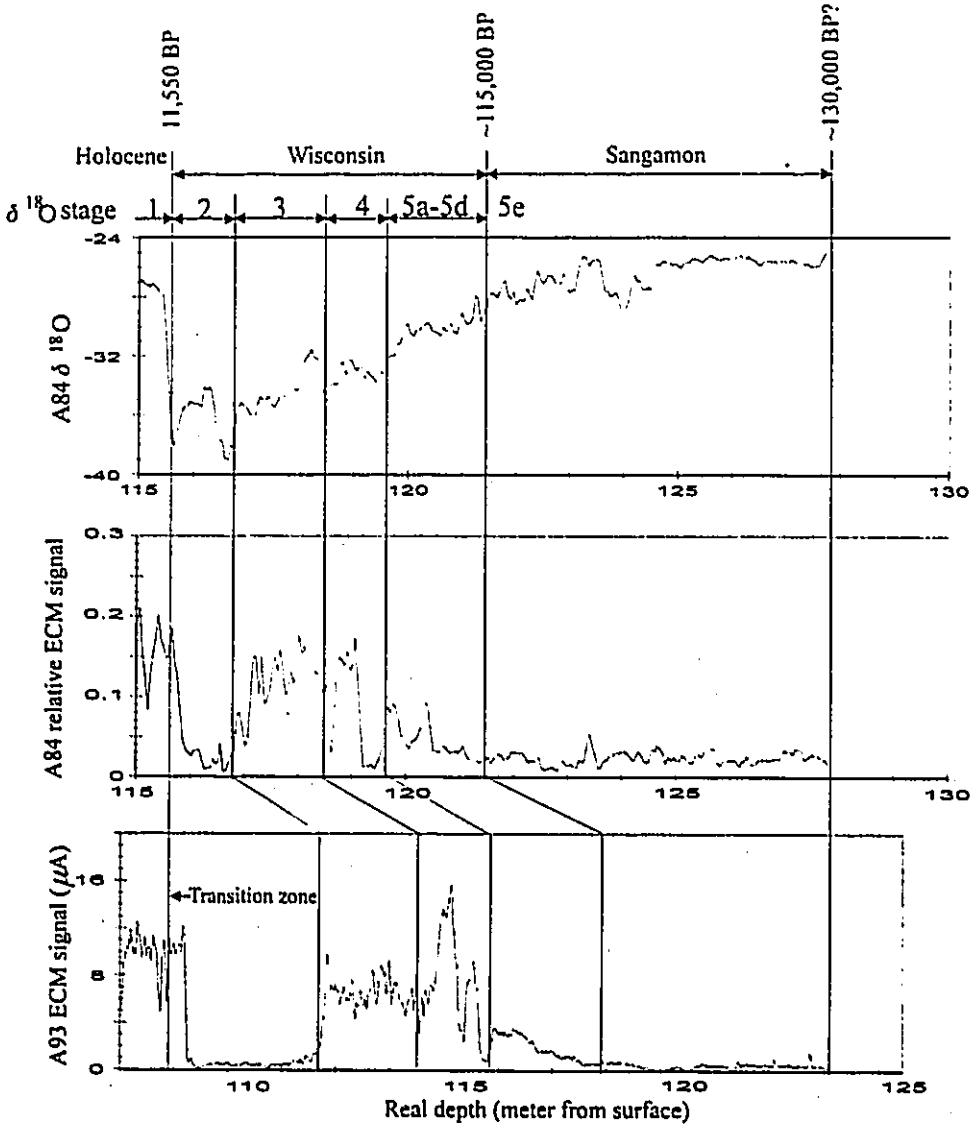

Figure 25. The bottom part of ECM results from the A93 ice cores. A84 $\delta^{18}O$ and ECM data are from Fisher et al. (1995). Climate sections are estimated based on $\delta^{18}O$ (Fisher and Koerner, 1986; Fisher, 1987; Koerner, 1989).

this silty layer is characteristic of the basal ice over much of the hill bedrock underlying the core site and extends for more than 1 km around that hill (Walford and Harper, 1981). Koerner (1989) found the morphology of the grains in this dirty ice was consistent with a history of basal melt followed by freeze-on at the bed of the ice cap. In this case, the dirty ice may be older than the last interglacial so that the debris was picked up by following pressure melting upstream along a palaeo-flowline when the ice was about 200 m thicker. However, present work (Koerner, 1989) suggests that the ice may be interglacial in origin and the dirt may have been blown onto the ice cap when it was small, which implies that the ice which survived from the early parts of the last interglacial period in the High Arctic could be little, if any. Some further special age dating such as ^{36}Cl is needed for the true age of the bottom ice to be more precisely determined.

5. Conclusion

1. ECM is a high resolution, fast, economical and an easily performed field method for establishing time horizons and transitions in ice cores. Its onsite operation can allow the quick location of specific volcanic events.

2. More than one ECM profile should be used in order to clearly identify certain specific events. Single ECM series risk missing signals on lower amplitude events like the Krakatoa eruption.

3. ECM signals from prepared and unprepared ice core surfaces are very similar even though detailed ECM signal differences exist. The correlation coefficient between the two ECM series of whole length ice cores from prepared and unprepared surfaces is 0.842, which suggests that ECM may be carried out immediately on mechanically recovered ice cores without creating a new surface, if care is being taken during the core handling and ECM processing. Correlation analysis of high resolution ECM records from the A93.1 prepared and unprepared surfaces over the last 250 years show that 10 to 30% the variability could not be explained, which is suggested to be mainly due to the total ECM methodological noise.

4. Ice cores taken only two metres apart have very similar ECM trends with similar locations of major ECM peaks. The correlation analysis gives a coefficient of 0.644 between the two whole length ice cores. Correlation analysis of high resolution ECM records from the A93.1 and A93.2 unprepared surfaces over the last 250 years gives a 30 to 50% variability. This suggests that there is a combined drift/melt noise contribution of 20% variability on top of the total ECM methodological noise for cores this close together.

5. Results from two similar ECM systems are highly cross correlated, virtually the same. In other words, the variability produced by the different similarly designed ECM systems is extremely small compared to the signal. This suggests that ECM results from different ECM systems could be comparable if the two ECM systems are similarly designed.

6. Review of multiple ice core records including $\delta^{18}O$, ECM and melt percentage, suggests that ice on the Agassiz Ice Cap of Canadian High Arctic is continuous from present to the early Holocene. However, a 100% melt percentage, high $\delta^{18}O$ noise and the discontinuities of $\delta^{18}O$ in the early Holocene suggests that there is some ice missing for the early Holocene period.

For further studies, I would like to suggest that 1). ECM results from the A93.1 and A93.2 cores be analysed by other statistical methods in order to better distinguish the signal and noise; 2). different voltage application between the electrodes to investigate the behaviour of different ions in the ice core be carried out in order to further dig into ECM method. I feel that there could be a possibility to separate the electrical different conductivity contribution from different valent ions by controlling the ion discharge via different voltage application; and 3). trace metals, greenhouse gases and other pollutants, such as acids (major anions), in the Canadian High Arctic ice caps be further investigated in a more detailed mode. It could greatly help to understand pollution history, climate variability or climate change, et al. in northern hemisphere.

6. References

Alley, R. B., D. A. Meese, C. A. Shuman, A. J. Gow, K. C. Taylor, P. M. Grootes, J. W. C. White, M. Ram, E. D. Waddington, P A. Mayewski and G. A. Zielinski. 1993. Abrupt increase in Greenland snow accumulation at the end of the Younger Dryas event. Nature 362, 527-529.

Bard E. , B. Hamelin, R. G. Fairbanks and A. Zindler. 1990. Calibration of the ^{14}C

timescale over the past 30,000 years using mass spectrometric U/Th ages from Barbados corals. Nature 345, 405-410.

Barnola J. M., D. Raynaud, Y. S. Korotkevich, and C. Lorius. 1987. Vostok ice core provides 160, 000 year record of atmospheric CO_2. Nature 329, 408-414.

Barnola J. M., D. Raynaud, A. Neftel, and H. Oeschger. 1983. Comparison of CO_2 measurements by two laboratories of air from bubbles in polar ice. Nature 303, 410-412.

Berner, W, B. Stauffer and H. Oeschger. 1978. Past atmospheric composition and climate: Gas parameters measured on ice cores. Nature 276, 53-55.

Bond, G., W. Broecker, S. Johnsen, J. McManus, L. Labeyrie, J. Jouzel and G. Bonani. 1993. Correlations between climatic records from North Atlantic sediments and Greenland ice. Nature 365, 143-147.

Boulton G. S. 1993. Two cores are better than one. Nature 366, 507-508.

Bourgeois J. C. 1986. A pollen record from the Agassiz Ice Cap, northern Ellesmere Island, Canada. Boreas 15(4), 345-354.

Camp P. R.; W. Kiszenick and D. A. Arnold. 1967. Electrical conduction in ice. Rept. 198, U.S. Army Cold Regions Research and Engineering Laboratory, September 1967.

Chappellaz J., T. Blunier, D. Raynaud, J. M. Barnola, J. Schwander and B. Stauffer. 1993. Synchronous changes in atmospheric CH_4 and Greenland climate between 40 and 8 kyr BP. Nature 366, 443-445.

Clausen H. B. and C. U. Hammer. 1988. The Laki and Tambora eruptions as revealed in Greenland ice cores from 11 locations. Annals of Glaciology 10, 16-22.

Clausen H. B., Gundestrup N. S., Johnsen S. J., Bindschadler R. and J. Zwally. 1988. Glaciological investigations in the Crete area central Greenland: a search for a new deep-drilling site. Annals of Glaciology 10, 10-15.

Crowlay T. J., T. A. Criste and N. R. Smith. 1993. Reassessment of Crete (Greenland) ice core acidity/volcanism link to climate change. Geophysical Research Letters 20, No. 3, 209-212.

Dansgaard W. and S. J. Johnsen. 1969. A flow model and a time scale for the ice core

from Camp Century, Greenland. Journal. of Glaciology 8, No. 53, 215-223.

Dansgaard W., S. J. Johnsen, H. B. Clausen and N. S. Gundestrup. 1973. Stable Isotope Glaciology. Meddelelser om Gronland. 197(2), 1-53.

Dansgaard, W., S. J. Johnsen, H. B. Clausen, D. Dahl-Jensen, N. S. Gundestrup, C. U. Hammer, C. S. Hvidberg, J. P. Steffensen, A. E. Sveinbjornsdottir, J. Jouzel and G. Bond. 1993. Evidence for general instability of past climate from a 250-kyr ice-core record. Nature 364, 218-220.

Dawson A. G.. 1992. Ice Age Earth: Late Quaternary Geology and Climate. Routledge, London.

Fisher, D. A. 1976. A study of two $\delta^{18}O$ records from Devon Ice Cap, Canada, and comparison of them to Camp Century $\delta^{18}O$ record, Greenland. (Ph. D. thesis): University of Copenhagen, Copenhagen, 287 p.

Fisher D. A. and R. M. Koerner. 1979. Some aspects of climatic change in the high Arctic during the Holocene as deduced from ice cores. In: Quaternary Paleoclimate.

Edited by W. C. Mahaney. Norwich, Geoabstracts, 249-271.

Fisher D. A., R. M. Koerner, W. S. B. Paterson, W. Dansgaard, N. Gundestrup and N Reeh. 1983. Effect of wind scouring on climatic records from ice-core oxygen-isotope profiles. Nature 301, 205-209.

Fisher D. A. and Koerner, R. M. 1983. Ice-core study: A climatic link between the past, present and future; in Climatic Change in Canada 3, C. R. Harington (ed); National Museum of National Sciences, Syllogeous 49, 50-69.

Fisher D. A. and B. T. Alt, 1985. A global oxygen isotope model - semi-empirical, zonally averaged. Annals of Glaciology 7, 117-124.

Fisher D. A., N. Reeh, and H. B. Clausen. 1985. Stratigraphic noise in time series derived from ice cores. Annals of Glaciology 7, 76-83.

Fisher D. A. and Koerner R. M. 1986. On the special rheological properties of ancient microparticle-laden Northern Hemisphere ice as derived from bore-hole and core measurements. Journal of Glaciology 32(112) 501-510.

Fisher D. A. 1987. Enhanced flow of Wisconsin ice related to solid conductivity through strain history and recrystallization. in: The Physical Basis of Ice Sheet Modelling (Proceedings of the Vancouver Symposium, August 1987). IAHS Publ. no. 170, 45-51.

Fisher D.A. and Koerner R. M. 1988. The effects of wind on $\delta^{18}O$ and accumulation give an inferred record of seasonal δ amplitude from the Agassiz Ice Cap, Ellesmere Island Canada. Annals of Glaciology 10, 34-37.

Fisher D. A. 1990. A zonally-averaged stable isotope model coupled to a regional variable-elevation stable-isotope model. Annals of Glaciology 14, 65-71.

Fisher D. A. 1991. Remarks on the deuterium excess in precipitation in cold regions. Tellus. 43B, 401-407.

Fisher D. A. 1992. Stable isotope simulations using a regional stable isotope model coupled to a zonally averaged global model. Cold Regions Sciences and Technology 21, 61-77.

Fisher D. A. 1992. Possible ice-core evidence for a fresh melt water cap over the Atlantic

Ocean in the Early Holocene. in: NATO ASI series vol 12 "The Last Deglaciation: Absolute and Radiocarbon Chronologies", editors E. Bard and W. S. Broecker. 267-293.

Fisher D. A. and R. M. Koerner. 1994. Signal and noise in four ice-core records from Agassiz Ice Cap, Ellesmere Island, Canada: details of the last millennium for stable isotopes, melt and solid conductivity. Holocene. 4(2), 113-120.

Fisher D. A., R. M. Koerner and N. Reeh. 1995. Holocene climatic records from Agassiz Ice Cap, Ellesmere Island, NWT, Canada. The Holocene, 5,1, 19-24.

Flint, R. F. 1971. Glacial and Quaternary Geology. John Wiley and Sons, New York, 892pp.

Grant D. R. 1989. Quaternary geology of the Atlantic Appalachian region of Canada. in Chapter 5 of Quaternary Geology of Canada and Greenland, R.J. Fulton (ed), Geological Survey of Canada, Geology of Canada, No. 1, 391-440.

Greenland Ice-core Project (GRIP) Members. 1993. Climate instability during the last interglacial period recorded in the GRIP ice core. Nature 364, 203-207.

Grootes P. M., M. Stuiver, J.W.C. White, S. Johnsen and J. Jouzel. 1993. Comparison of oxygen isotope records from the GISP2 and GRIP Greenland ice cores. Nature 366, 552-554.

Hall, K. 1982. Rapid deglaciation as an initiator of volcanic activity: a hypothesis. In: Earth Surface Processes and Landforms, 7, 45-51.

Hammer C. U., Clausen H. B. and Dansgaard W. 1980. Greenland ice sheet evidence of post glacial volcanism and its climatic impact. Nature, 288 (5788), 230-235.

Hammer C. U., 1980. Acidity of polar ice cores in relation to absolute dating, past volcanism, and radioechoes. Journal of Glaciology 25, No. 92, 359-372.

Hammer C. U. 1984. Traces of Icelandic eruptions in the Greenland ice sheet. Jökull 34, 51-65.

Hammer C. U., 1985. The influence on atmospheric composition of volcanic eruptions as derived form ice-core analysis. Annals of Glaciology 7, 125-129.

Hammer C. U. 1989, Dating by physical and chemical seasonal variations and reference

horizons. In: The Environmental Record in Glaciers and Ice Sheets eds. H. Oeschger and C. C. Langway. Jr., 99-121.

Hansson M. E. 1994. The Renland ice core. A northern Hemisphere record of aerosol composition over 120,000 years. Tellus, 46B, 390-418.

Hattersley-Smith, G. 1972, Climatic change and related problems in N. Ellesmere Island, N. W.T., Canada, in Vasari, Y., Hyvarinen, H. and Hicks, S., eds., Climatic Changes in Arctic Areas during the last Ten Thousand Years. (In: Proceedings of the Oulanda and Keva symposium, Finland, October. 1971). Acta Universitat, Oulu University, Oulu, Finland, No. 3, 137-148.

Johnsen, S. J. 1977. Stable isotope homogenization of polar firn and ice, In: Isotopes and Impurities in Snow and Ice. (In: Proceedings of the Grenoble Symposium, August-September 1975). IAHS Publ. No. 118, 210-219.

Johnsen S. J., W. Dansgaard and J. W. C. White, 1989. The origin of Arctic precipitation under present and glacial conditions. Tellus, 41B, 452-468.

Johnsen S. J., H. B. Clausen, W. Dansgaard, K. Fuhrer, N. Gundestrup, C. U. Hammer, P. Iversen, J. Jouzel, B. Stauffer, and J. B. Steffensen. 1992. Irregular glacial interstadials recorded in a new Greenland ice core. Nature 359, 311-313.

Junge C. E. 1977. Processes responsible for the trace content in precipitation. International Association of Hydrological Sciences Publication 118 (General Assembly of Grenoble 1975 - Isotopes and Impurities in Snow and Ice): 63-77.

Keeling C. D., R. B. Bacastow, A. F. Carter, S. C. Piper, T. P. Whorf, M. Heimann, W. G. Mook, and H. Roeloffzen, 1989. A three-dimensional model of atmospheric CO_2 transport based on observed winds: 1. Analysis of observational data. In: Aspects of climate variability in the Pacific and Western Americas (Ed. D. H. Peterson), Geophysical Monograph 55, 165-236. American Geophysical Union, Washington, DC, 1989.

Koerner R. M. 1977. Devon Island ice cap; core stratigraphy and paleoclimate. Science 196, 15-18.

Koerner R. M. 1979. Accumulation, ablation and oxygen isotope variations on the Queen

Elizabeth Islands ice caps, Canada. Journal of Glaciology. 22(86), 25-41.

Koerner R. M. 1989. Ice core evidence for extensive melting of the Greenland ice sheet in the Last Interglacial. Science 244, 964-968.

Koerner R. M. 1989. Queen Elizabeth Islands Glaciers; in Chapter 6 of Quaternary Geology of Canada and Greenland, R.J. Fulton (ed), Geological Survey of Canada, Geology of Canada, 1, 464-477.

Koerner R. M., D. A. Fisher and W. S. B. Paterson. 1987. Wisconsin and pre-Wisconsin ice thicknesses on Ellesmere Island Canada: Inferences from ice cores. Canadian Journal of Earth Sciences, 24, 296-301.

Koerner R. M., Bourgeois J. C. and D. A. Fisher. 1988. Pollen analysis and discussion of time-scales in Canadian ice cores. Annals of Glaciology, 10, 85-91.

Koerner R. M. and D. A. Fisher. 1990. A record of Holocene summer climate from a Canadian high-Arctic ice core. Nature 343 (6259), 630-631.

Lamb, H. H. 1982. Climate, History and the Modern World. Methuen, London, 387pp.

Lange, G.R., C.C. Langway Jr., and B.L. Hansen. 1959. Deep core drilling in glaciers: Proceedings of U.S. Army Science Conference, 1959, West Point, NY., 2, 97-107.

Langway C. C., Jr., H. B. Clausen and C. U. Hammer. 1988. An inter-hemispheric volcanic time-marker in ice cores from Greenland and Antarctica. Annals of Glaciology 10, 1-7.

Langway, C. C., Jr. and H. Oeschger, 1989. Introduction, in The Environmental Record in Glaciers and Ice Sheets. eds. H. Oeschger and C.C. Langway. Jr., 1-11.

Legrand M. and R. J. Delmas. 1987. A 220-year continuous record of volcanic H_2SO_4 in the Antarctic ice sheet. Nature 327, 671-676.

Lowe, J. J. and Walker, 1984. Chapter 6: Approaches to Quaternary stratigraphy and correlation. In: Reconstructing quaternary environments. Longman, New York.

Mayewski, P. A., L. D. Meeker, S. Whitlow, M. S. Twickler, M. C. Morrison, R. B. Alley, P. Bloomfield and K. Taylor. 1993. The Atmosphere During the Younger Dryas. Science 261, 195-197.

Muller, F., 1966. Evidence of climatic fluctuations on Axel Heiberg Island, Canadian Arctic Archipelago, in Fletcher, J. O., ed., Proceedings of the Symposium on the Arctic heat budget and atmospheric circulation: Santa Monica, Calif., Rand Corp.,136-156.

Neftel, A., M. Andree, J. Schwander, B. Stauffer and C.U. Hammer. 1985. Measurements of a kind of DC conductivity on cores from Dye 3. In: Greenland Ice Cores: Geophysics, Geochemistry, and the Environment (ed. by C. C. Langway, Jr., H. Oeschger & W. Dansgaard), 32-38. Geophysical Monograph 33, American Geophysical Union, Washington, D.C., USA.

Paterson W. S. B. 1981. The Physics of Glaciers. Pergamon Press. 380 pages.

Paterson, W. S. B., R. M. Koerner, D. A. Fisher, S. J. Johnsen, H. R. Clausen, W. Dansgaard, P. Bucher and H. Oschger. 1977. An oxygen isotope climatic record from the Devon Island Ice Cap, Arctic Canada; Nature 266, 508-511.

Rampino, M. R., S. Self and R. W. Fairbridge, 1979. Can rapid climatic change cause volcanic eruptions? Science, 206, 826-829.

Reeh N. 1988. A flow-line model for calculating the surface profile and the velocity, strain rate and stress fields in an ice sheet. Journal of Glaciology, vol 34(116), 46-54.

Ritchie J. C., L. C. Cwynar, and R. W. Spear, 1983. Evidence from north-west Canada for an early Holocene Milankovitch thermal maximum. Nature 305, 126-128.

Schwander J., A. Neftel, H. Oeschger and B. Stauffer. 1983. Measurement of direct current conductivity on ice sample for climatological applications. Journal of Physical Chemistry, 87, 4157-4160.

Sejrup, H.-P, J. Sjoholm, H. Furnes, I. Beyer, L. Eide, E. Jansen and Mangerud. 1989. Quaternary tephrachronology on the Iceland plateau, north of Iceland. Journal of Quaternary Science, 4, 109-114.

Shackleton, N. J., 1987. Oxygen isotopes, ice volume and sea level. Quaternary Science Reviews, 6, 183-190.

Shaw G. E., 1989. Aerosol transport from sources to ice sheets. In: The environmental record in glaciers and ice sheets. eds. Oeschger H. and C.C. Langway. Jr. John Wiley

and Sons, New York. 13-27.

Taylor K., R. Alley, J. Fiacco, P. Grootes, G. Lamorey, P. Mayewski and M. J Spencer. 1992. Ice-core dating and chemistry by direct-current electrical conductivity. Journal of Glaciology 38, No. 130, 325-332 .

Taylor K. C., G. W. Lamorey, G. A. Doyle, R. B. Alley, P. M. Grootes, P. A. Mayewski, J. W. C. White and L. K. Barlow. 1993. The 'flickering switch' of late Pleistocene climate change. Nature 361, 432-436.

Taylor K. C., C. U. Hammer, R. B. Alley, H. B. Clausen, D. Dahl-Jensen, A. J. Gow, N. S. Gundestrup, J. Kipfstuhl, J. C. Moore and E. D. Waddington. 1993. Electrical conductivity measurements from the GISP2 and GRIP Greenland ice cores. Nature 366, 549-552.

Wagenbach D. , K. O. Münnich, U. Schotterer and H. Oeschger 1988. The anthropogenic impact on snow chemistry at Colle Gnifetti, Swiss Alps. Annals of Glaciology 10, 183-187.

Wahlen M., D. Allen, B. Deck and A. Herchenroder, 1991. Initial measurements of CO_2 concentrations (1530 to 1940 AD) in air occluded in the GISP2 ice core from central Greenland. Geophysical Research Letters, v.18, no.8, 1457-1460.

White J. W. C. 1993. Don't touch that dial. Nature 364, 186.

WCD. 1992. World Climate Disc, Global Climate Change Data. CD ROM. Chadwyck-Healey Ltd. Cambridge UK. Compilations by Climatic Research Unit University of East Anglia and The Hadley Centre for Climatic Prediction and Research, Meteorological Office, UK.

Zecca A. and R. S. Brusa. 1991. The missing part of the greenhouse effect. IL Nuovo UMENTO. vol. 14c, N.5, 523-532.

Zheng J., A. Kudo, D. A. Fisher, R. M. Koerner, M. Gerasimoff and E. Blake. 1995. Solid electric conductivity (ECM) from four Agassiz Ice Cores, Ellesmere Island, NWT, Canada; Volcanism and Climate related variations over the last 120 thousand years. Submitted to J. of Holocene.